N 62 65958 ARR Nov. 1942

NATIONAL ADVISORY COMMITTEE FOR AERONAUTICS

WARTIME REPORT

ORIGINALLY ISSUED

November 1942 as
Advance Restricted Report

THE EFFECT OF EXHAUST-STACK SHAPE ON THE DESIGN AND PERFORMANCE OF THE INDIVIDUAL CYLINDER EXHAUST-GAS JET-PROPULSION SYSTEM

By L. Richard Turner and Leroy V. Humble

Aircraft Engine Research Laboratory
Cleveland, Ohio

NACA

WASHINGTON

NATIONAL ADVISORY COMMITTEE FOR AERONAUTICS

ADVANCE RESTRICTED REPORT

THE EFFECT OF EXHAUST-STACK SHAPE ON THE DESIGN AND PERFORMANCE OF THE INDIVIDUAL CYLINDER EXHAUST-GAS JET-PROPULSION SYSTEM

By L. Richard Turner and Leroy V. Humble

SUMMARY

Tests were made on a single-cylinder, air-cooled engine to determine the effect of several different exhaust-stack shapes on the design and performance of the individual cylinder exhaust-gas jet-propulsion system.

The results of the investigation indicate that the presence of smooth bends in the exhaust stack or an increase in length up to approximately 4 feet have a very small effect on the total performance obtainable at a given set of operating conditions. Tests with a straight stack 9 feet in length indicate that there is a limiting value of exhaust-stack length beyond which the effect on engine power is appreciable.

Curves are given for use in designing nozzles for various exhaust-stack shapes and for predicting the gain in thrust horsepower that may be expected at various operating conditions.

INTRODUCTION

In reference 1 there was developed a method of determining the effect of exhaust-stack discharge area on engine power and exhaust-gas jet thrust. Curves are given for designing exhaust-stack nozzles and for predicting the jet thrust obtainable at various operating conditions. It was found that a considerable gain in thrust horsepower could be obtained by the utilization of exhaust-gas jet thrust. The tests were made on a single-cylinder engine with a single straight exhaust stack 25 inches in length.

In actual installations it is seldom possible to use straight stacks, and various bends must be introduced into the exhaust system. The exhaust-stack length will also vary with different installations.

This report presents the results of tests of an 1820-G single-cylinder engine to determine the effects of nozzle area and stack shape on engine power and exhaust-gas jet thrust. The considerable amount of data obtained has been condensed into relatively few curves for use in designing nozzles for various stack shapes and for predicting the gain in thrust horsepower to be expected at various operating conditions.

The tests were made at the Langley Memorial Aeronautical Laboratory during the period from June to December 1941.

ANALYSIS

Method of Determining the Effect of Nozzle Area on Exhaust-Gas Jet Thrust and Engine Power

It is shown in reference 1 that the thrust produced by the discharge of exhaust gas from a short straight stack may be represented by a single curve regardless of variation in nozzle discharge area or engine conditions if F/M_e is plotted against p_oA/M_e. The quantity F/M_e is the mean exhaust-gas jet velocity and is designated $\overline{V}_e$. Thus

$$\overline{V}_e = F/M_e = f_1(p_oA/M_e) \qquad (1)$$

where

F average exhaust-gas jet thrust, pounds

M_e average mass rate of flow of exhaust gas, slugs per second

p_o atmospheric pressure, pounds per square foot

A exhaust-nozzle area, square feet

In the case of exhaust systems of such shape that resonance effects are appreciable, factors not uniquely dependent on $p_o A/M_e$ may be expected to be important in determining $\overline{V}_e$. In the case of stacks free of resonance effects, some difference in the variation of $\overline{V}_e$ with $p_o A/M_e$ may be expected when the exhaust-stack shape is sufficiently changed. For example, the discharge process from exhaust stacks will tend to be slowed down by an increase in stack volume with a consequent reduction in $\overline{V}_e$.

The effect of nozzle area on engine power is shown in reference 1 in the following manner:

The ratio of indicated mean effective pressure to inlet manifold pressure is used as a measure of engine power. This ratio ϕ is a function of p_o/p_m, $v_d n/A$, and engine speed.

Thus

$$\phi = \frac{\text{imep}}{p_m} = f_2\left(\frac{p_o}{p_m}, \frac{v_d n}{A}, n\right) \qquad (2)$$

where

imep indicated mean effective pressure, pounds per square foot

p_m intake manifold pressure, pounds per square foot

v_d displacement volume of engine, cubic feet

n engine speed, revolutions per second

It is convenient to represent the loss in engine power resulting from restriction of the exhaust-stack exit area by the quantity $\Delta\phi$. Thus

$$\Delta\phi = \phi - \phi_o \qquad (3)$$

where ϕ is for a given nozzle area at a given engine speed, intake manifold pressure and temperature, and atmospheric pressure, and ϕ_o is for the same stack at the same operating conditions but with no nozzle restriction. The quantity $\Delta\phi$ is principally a function of p_o/p_m and $v_d n/A$.

Method of Determining the Effect of Nozzle Area and Stack Shape on Total Performance

The total thrust horsepower when exhaust-gas jet thrust is utilized is given by the relation

$$P_T = \eta_P P + \frac{M_e \bar{V}_e V}{550} \tag{4}$$

where

P_T total thrust horsepower

P brake horsepower of engine

η_P propeller efficiency

V airplane velocity, feet per second

In the region where reduction in nozzle area causes a loss in engine power, the net gain in thrust power is given by ΔP_T where

$$\Delta P_T = \eta_P (P - P_o) + \frac{M_e \bar{V}_e V}{550} \tag{5}$$

where P_o is the brake horsepower obtained from the engine with the unrestricted stack, and P is the value with the constricted nozzle.

Since P and P_o each apply for the same engine speed, manifold pressure, manifold temperature, and atmospheric pressure the mechanical friction is the same for each case and, except for variations in supercharger power, $P-P_o$ can be replaced by $I-I_o$ where I and I_o are the indicated horsepowers corresponding to P and P_o, respectively. But

$$I = \frac{\text{imep } v_d \, n}{2 \times 550} = \phi \frac{p_m \, v_d \, n}{2 \times 550}$$

Thus

$$I - I_o = \frac{p_m \, v_d \, n}{2 \times 550} \Delta\phi$$

and M_e is given by the relation

$$M_e = \frac{p_m \, v_d \, n}{2 \, R \, T_m} (1 + f) \, \eta_v$$

where

f fuel-air ratio

η_v volumetric efficiency of the engine

T_m intake manifold temperature, $^{\circ}F$ absolute

R gas constant for air, foot-pounds per slug $^{\circ}F$

If $\Delta\phi_T$ is defined by the relation

$$\Delta\phi_T = \frac{2 \times 550}{p_m \, v_d \, n \, \eta_P} \Delta P_T$$

equation (5) becomes

$$\Delta\phi_T = \Delta\phi + \frac{(1+f)}{R \, T_m} \eta_v \, \overline{V}_e \, \frac{V}{\eta_P} \qquad (6)$$

The quantity $\Delta\phi_T$ can be considered as a net increase in the mean effective pressure of the engine divided by the intake manifold pressure on the assumption that the jet thrust power, represented by $\left(\frac{1+f}{R \, T_m} \eta_v \, \overline{V}_e \, \frac{V}{\eta_P}\right)$, is credited to the engine power.

If $\Delta\phi_T$ is considered to be due to an effective mean exhaust-gas jet velocity $(\overline{V}_e)_{eff}$, it becomes

$$\Delta\phi_T = \frac{1+f}{R \, T_m} \eta_v \, \frac{V}{\eta_P} \, (\overline{V}_e)_{eff} \qquad (7)$$

Substituting equation (7) in equation (6) and solving for $(\overline{V}_e)_{eff}$ gives

$$(\bar{V}_e)_{eff} = \frac{R\ T_m}{(1+f)\eta_v} \frac{\eta_p}{V} \Delta\phi + \bar{V}_e \qquad (8)$$

It has previously been shown that $\Delta\phi$ and η_v are functions mainly of p_o/p_m and $v_d n/A$ and that $\bar{V}_e$ is a function of $p_o A/M_e$. But

$$\frac{p_o A}{M_e} = \frac{p_o}{p_m} \times \frac{A}{v_d n} \times \frac{2\ R\ T_m}{(1+f)\eta_v} \qquad (9)$$

Thus, if p_o/p_m and V/η_p are constant, $\Delta\phi$ and η_v and consequently $(\bar{V}_e)_{eff}$ may be considered functions of $p_o A/M_e$.

APPARATUS

Thrust measurements were made with the altitude thrust target described in detail in reference 1. The only change in this device was the installation of a water spray for cooling the inner tank.

The equipment for determining the effect of exhaust discharge area on engine power was also essentially the same as described in reference 1. The only variation was the use of several differently shaped exhaust stacks. (See fig. 1.) These stacks included (a) an offset or S-shape, (b) a 90° bend, (c) a 180° bend, (d) a short straight stack having a closed branch faired into it, and two straight stacks, 44 inches and 9 feet in length. Each stack had an inside diameter of $2\frac{5}{16}$ inches and was provided with flanges for mounting between the engine and the exhaust tank.

A sketch giving the main dimensions of the stacks is shown in figure 2. In some cases it was necessary to add short extensions to the stack as an aid in changing nozzles. These extensions are shown by dashed lines in figure 2.

The nozzles used in the tests were 5 inches long and consisted of a 3-inch tapered section faired into 1-inch

straight sections at each end. One nozzle was made with its exit end cut in a plane making an angle of 30° with the nozzle axis. (See fig. 3.)

TEST PROCEDURE

The test procedure for both thrust and power determinations was essentially the same as described in reference 1.

The following engine conditions were maintained in all the tests. The fuel-air ratio was held between 0.079 and 0.081; the engine speed was held to within ±10 rpm of the desired value, the oil-out temperature was held between 140° F and 160° F; and the cooling-air pressure drop was held between 17 and 20 inches of water.

Thrust determinations were made with the 180° bend and the branched stack. Each stack was tested at engine speeds of 1300, 1500, 1700, 1900, and 2100 rpm with several different nozzle areas. In general, for each nozzle area the engine was operated over the following range of conditions:

(a) Intake manifold pressure constant at 30 inches of mercury absolute and thrust target pressures varied from 12 to 30 inches of mercury absolute.

(b) Intake manifold pressure varied from 24 to 30 inches of mercury absolute and thrust target pressure constant at 30 inches of mercury absolute.

The weight rate of flow of exhaust gas was determined by a calibrated orifice in the air-intake line and a rotameter in the fuel line.

In addition to the foregoing tests, thrust determinations were made with a 20-inch straight stack and the beveled nozzle. The thrust was first determined with the beveled nozzle exit. The beveled portion was then cut off so the nozzle exit was normal to its axis, and thrust determinations were again made to determine the effect of the bevel on thrust. The plane of the beveled nozzle was vertical during the tests, and only the axial component of the velocity was determined.

All the stacks were tested for their effect on power.

Each stack, except the 9-foot stack, was tested as follows: With a given nozzle exit area, runs were made at engine speeds of 1300, 1500, 1700, 1900, and 2100 rpm. At each speed the intake manifold pressure was held at approximately 30 inches of mercury absolute and the exhaust tank pressure was varied from 12 to 30 inches of mercury absolute in steps of approximately 3 inches of mercury. Several different nozzle areas were tested at each engine speed.

The 9-foot stack was tested by holding the ratio p_o/p_m constant, while the engine speed was varied from 1300 to 2100 rpm in steps of approximately 100 rpm. The engine power was determined at each speed. Several nozzle areas were tested over the speed range at $p_o/p_m = 0.4$, 0.7, and 1.0.

Motoring friction was determined with the unrestricted S-shaped stack over the range of engine speeds with sea-level intake and exhaust pressures. The values obtained were found to agree with those for the 25-inch straight stack. The friction power as determined for the 25-inch straight stack was used in all cases to obtain the indicated mean effective pressure.

DISCUSSION OF RESULTS

The Effect of Nozzle Area and Stack Shape on Exhaust-Gas Jet Thrust

Figure 4(a) shows the variation of the exhaust-gas jet thrust F/M_e as represented by $\overline{V}_e$, with p_oA/M_e for the exhaust stack having a 180° bend. Inspection of the figure shows that the data agree, in general, with the curve obtained for the 25-inch straight stack in reference 1. The nozzle with an area of 0.91 square inch is seen to give somewhat smaller values of $\overline{V}_e$ than would be expected from the curve and other considerations. This result is believed to be due to experimental error because intermittent afterburning occurred in the thrust tank during this run and made an accurate reading of the thrust and back pressure difficult. This difficulty was eliminated in the other runs by cooling the thrust target with a water spray. Inasmuch as stacks having bends of less than 180° may be expected to have correspondingly less effect on

exhaust-gas thrust, it is believed that the curve of $\overline{V}_e$ against $p_o A/M_e$ for the 25-inch stack may be used to predict the thrust obtainable with all single stacks having smooth bends of various amounts.

Figure 4(b) shows the variation of $\overline{V}_e$ with $p_o A/M_e$ for the branched stack. The data do not fit the curve for the 25-inch stack but give somewhat smaller values of $\overline{V}_e$ for a given value of $p_o A/M_e$. This difference is probably due to the influence of the closed branch on the exhaust-discharge process. It is not certain that the thrust as obtained in these tests will apply when both legs of the branch are used, as in a multicylinder installation. The uncertainty is increased if the two legs are connected to cylinders with overlapping exhaust-valve timing.

Figure 4(c) shows the effect of a beveled nozzle exit on thrust. Data are given for a straight stack 20 inches long and the nozzle with the beveled exit. Corresponding data are also shown for the same stack and nozzle after the beveled portion of the nozzle had been cut off until the exit was normal to the nozzle axis. The beveled exit gave slightly smaller values of $\overline{V}_e$ than the normal exit for a given value of $p_o A/M_e$.

The Effect of Nozzle Area and Stack Shape on Over-All Performance for the S-Shape, the 90° Bend, and the 180° Bend

Figures 5(a), 5(b), and 5(c) show the optimum values of $v_d n/A$ plotted against p_o/p_m for the S-shape, the 90° bend, and the 180° bend, respectively. These values were obtained by plotting $\Delta\phi_T$ as determined by equation (6) against $v_d n/A$ at constant values of p_o/p_m and V/η_p. The values of $v_d n/A$ corresponding to the maximums of curves faired through the data were considered the optimum. They are the values for which the net gain in thrust horsepower is a maximum at the given values of p_o/p_m and V/η_p. The curves for $\Delta\phi = 0$ represent the values of $v_d n/A$ at which the engine just begins to lose power. They were taken by inspection from the curves of $\Delta\phi$ against $v_d n/A$.

Inspection of figure 5 shows that the optimum value of $v_d n/A$, for a constant value of p_o/p_m, increases with V; thus, for a given engine and engine speed, the correct nozzle area will decrease as V increases. The optimum values of $v_d n/A$ decrease with the ratio p_o/p_m indicating that, in general, the required nozzle area will increase with the critical altitude. A comparison of figures 5(a), 5(b), and 5(c) shows that, for constant values of p_o/p_m and V/η_P, the optimum values of $v_d n/A$ tend to decrease as the amount of bend in the stack increases. The optimum values for the S-shaped stack fall between the values for the 90° and the 180° bends. This variation apparently does not apply for the condition where $\Delta\phi = 0$, in which case the S-shaped stack allows slightly larger values of $v_d n/A$ than the other two stacks at the larger values of p_o/p_m.

Figure 6 shows $(\overline{V}_e)_{eff}$ as determined by equation (8) plotted against $p_o A/M_e$ at constant values of p_o/p_m for two values of V/η_P. Curves are given for the S-shaped bend, the 90° bend, and the 180° bend. These curves were computed on the basis of $T_m = 540°$ F absolute, $f = 0.08$, and a volumetric efficiency η_v at 2100 rpm. Volumetric efficiency was determined by the relation

$$\eta_v = \eta_{v_o} + \Delta\eta_v$$

where η_{v_o} was the value at 2100 rpm and $\Delta\eta_v$ was obtained from the appropriate curves of $\Delta\eta_v$ against $v_d n/A$. Values of $\Delta\phi$ were obtained from faired curves of $\Delta\phi$ against $v_d n/A$ and $\overline{V}_e$ was obtained from the curve of $\overline{V}_e$ against $p_o A/M_e$ for the 25-inch stack.

The thrust of the exhaust-gas jet as represented by the curve of $\Delta\phi = 0$ is seen to increase as $p_o A/M_e$ decreases. At each value of p_o/p_m and of airplane velocity V a value of $p_o A/M_e$ is reached where the curve $(\overline{V}_e)_{eff}$ branches from the curve $\Delta\phi = 0$. This value of $p_o A/M_e$ represents the point where the engine just begins to lose power for these conditions. As $p_o A/M_e$ is reduced from this value, the curve $(\overline{V}_e)_{eff}$ continues to increase slightly because the gain in jet

thrust power is larger than the loss in engine power. An optimum value of p_oA/M_e is finally reached at which $(\overline{V}_e)_{eff}$ is a maximum. As p_oA/M_e decreases beyond this point, the loss in engine power is greater than the gain in jet thrust power and $(\overline{V}_e)_{eff}$ decreases. Lines faired through the maximum values of $(\overline{V}_e)_{eff}$ are shown for two values of V/η_p.

Only a small change in the curves for $(\overline{V}_e)_{eff}$ is effected by a change in airplane speed from 200 to 350 miles per hour. This percentage change in V is much greater than any percentage change in η_v or T_m (from the values assumed in the preparation of fig. 6) that might be expected in practical operation. Equation (8) shows that a given percentage change in T_m or η_v has the same effect on $(\overline{V}_e)_{eff}$ as an equal change in V; thus, normal variations of T_m or η_v from the values assumed in preparing figure 6 should have only a small effect on the curves of $(\overline{V}_e)_{eff}$. Similarly, normal changes in fuel-air ratio will have only a small effect on $(\overline{V}_e)_{eff}$.

It is noted that, for large values of p_o/p_m, the curves of $(\overline{V}_e)_{eff}$ against p_oA/M_e are relatively flat near their maximum values and the nozzle area may vary considerably from its optimum value without greatly affecting the net gain in thrust power. For small values of p_o/p_m, $(\overline{V}_e)_{eff}$ is more sensitive to changes in p_oA/M_e and the nozzle area is more critical. The percentage range of area, however, remains nearly constant as p_o/p_m varies.

Figure 5 is convenient for determining the correct nozzle area for a given set of conditions. Figure 6 can be used to predict the gain in performance to be expected from the installation.

The method of using the curves is shown by the following example. Assume the following conditions:

Engine displacement volume, cubic inches	1800
Number of cylinders	14
Engine speed, rpm	2400
Brake horsepower	1100
Atmospheric pressure, inches Hg absolute	13.75
Intake manifold pressure, inches Hg absolute	43.00
Propeller efficiency	.85
Airplane velocity, miles per hour	350

Then $p_o/p_m = 13.75/43.0 = 0.32$.

If S-shaped stacks are used, the value of $v_d n/A$ corresponding to maximum performance is 145 (fig. 5(a)). The nozzle area per cylinder is given by

$$\text{Area} = \frac{v_d n}{145} = \frac{1800}{14 \times 1728} \times \frac{2400}{60} \times \frac{144}{145} = 2.96 \text{ square inches}$$

If a charge consumption of 2.4 pounds per second is assumed, $p_o A/M_e$ is given by

$$\frac{p_o A}{M_e} = 13.75 \times 0.491 \times 144 \times \frac{2.96}{144} \times \frac{14 \times 32.2}{2.4} = 3750 \text{ feet per second}$$

From figure 6(a) the corresponding value of $(\overline{V}_e)_{eff}$ is 2260 feet per second, and the net gain in thrust horsepower is given by

$$\Delta P_T = \frac{M_e (\overline{V}_e)_{eff} V}{550} = \frac{2.4}{32.2} \times \frac{2260}{550} \times 514 = 157.4 \text{ horsepower}$$

This value is 16.84 percent of the engine thrust horsepower. On the assumption that the airplane velocity varies as the cube root of the thrust horsepower, the increase in V is given by

$$\Delta V = 350 \left[\sqrt[3]{1.1684} - 1 \right] = 19 \text{ miles per hour}$$

The thrust horsepower of the jet alone is obtained from the curve $\Delta\phi = 0$ and is equal to P_J where

$$P_J = \frac{M_e \overline{V}_e V}{550} = \frac{2.4}{32.2} \times 2350 \times \frac{514}{550} = 163.5 \text{ horsepower}$$

The difference in thrust horsepower, 163.5 - 157.4 = 6.1, is due to the loss in engine power.

If the example is computed on the basis of the value of $v_d n/A$ at which the engine begins to lose power, the

required nozzle area is 3.54 square inches per cylinder, which is 19.6 percent larger than the area corresponding to maximum performance. The value of ΔV for this case is approximately 18.5 miles per hour. Although the difference in performance with the two nozzle areas is slight, an improvement in flame damping will possibly result from the use of the smaller nozzle area. It is evident from figure 6 that the nozzle area may be reduced to a value somewhat below the optimum with only a small effect on total performance.

Figure 7 shows the variation of the effective brake specific fuel consumption $(bfc)_{eff}$ with $v_d n/A$ for various values of p_o/p_m. The curves are based on data for the S-shaped stack and were computed for an airplane velocity of 350 miles per hour and a propeller efficiency of 0.85. Values of $(bfc)_{eff}$ were determined by the following relation

$$(bfc)_{eff} = (ifc)_o \left[\frac{\phi_o}{\phi_{b_o} + \Delta\phi_T}\right] \frac{\eta_v}{\eta_{v_o}}$$

where ϕ_o is for an engine speed of 2100 rpm and a given value of p_o/p_m; ϕ_{b_o} is the ratio $bmep/p_m$ for the same conditions; $\Delta\phi_T$ represents the net gain in thrust horsepower at a given value of $v_d n/A$; η_v represents the corresponding volumetric efficiency; η_{v_o} is the volumetric efficiency corresponding to ϕ_o and ϕ_{b_o}; and $(ifc)_o$ is the indicated specific fuel consumption for the unrestricted stack condition.

The value of $(ifc)_o$ was taken as 0.495 at $p_o/p_m = 1.0$, which corresponds to a brake specific fuel consumption of 0.55 for the same conditions. It was assumed to be constant for all values of p_o/p_m.

The value of ϕ_{b_o} was obtained by the relation

$$\phi_{b_o} = \phi_o - \phi_f - \phi_s$$

where ϕ_f is the ratio of friction mean effective pressure to intake manifold pressure $fmep/p_m$; fmep was taken as 0.1

imep at $p_o/p_m = 1.0$; ϕ_s is the ratio of supercharger mean effective pressure to intake manifold pressure smep/p_m computed on the basis of full throttle operation. In the computation of ϕ_s the adiabatic efficiency was taken as 0.65 and the gear efficiency was taken as 0.85.

The points for $\Delta\phi_T = 0$ in figure 7 represent the brake specific fuel consumption when no jet thrust is utilized. The points for $\Delta\phi_T$ = maximum represent the values of $v_d n/A$ corresponding to maximum performance. Maximum economy is obtained at the values of $v_d n/A$ corresponding to maximum performance.

The 90° bend and the 180° bend will give approximately the same gain in economy as the S-shaped stack for a given set of conditions.

The Effect of Stack Shape and Nozzle Area on Engine Power and Volumetric Efficiency for the S-Shaped, the 90° Bend, and the 180° Bend

The variation of ϕ and volumetric efficiency η_v with p_c/p_m for various nozzle areas at constant engine speeds is shown for the S-shaped stack in figures 8 and 9. The curves are similar to those obtained for the 25-inch stack (reference 1).

Values of $\Delta\phi$ as obtained from the faired curves in figure 8 are plotted against $v_d n/A$ in figure 10 for constant values of p_o/p_m. The values of ϕ for the nozzle having an area of 4.20 square inches represent the unrestricted-stack condition. There appears to be a smooth transition from the region of no loss in power to the region where a loss occurs. In reference 1 there was found a very sharp transition from no loss in power to the region where a loss occurred and the data for the 25-inch stack could be represented by a straight line intersecting the $\Delta\phi = 0$ line at a value of $v_d n/A$ corresponding to the point at which the engine just started to lose power. This difference in the variation of $\Delta\phi$ with $v_d n/A$ for the two stacks may be explained as follows: The bends in the S-shaped stack represent a

slight initial restriction so that with no nozzle restriction on the end of the stack a slightly larger effective value of $v_d n/A$ exists for this stack than for the 25-inch stack. Although the effective area is large enough that no loss in power is experienced, it is apparent that the addition of a nozzle with its attendant pressure drop will cause a loss in power with less decrease in area than for the straight stack. As the nozzle area decreases, the effect of the inherent stack restriction is decreased with the result that a gradual transition occurs. For greatly decreased nozzle areas the effect of initial restriction becomes negligible and the power loss approaches that for the straight stack.

The values of $v_d n/A$ at which the engine just begins to lose power were taken by inspection from figure 10 and are plotted against p_o/p_m in figure 5(a). They are represented by the curve $\Delta\phi = 0$. The corresponding curve for the 25-inch stack is also given in order to show the effect of bends on the value of $v_d n/A$ at which a loss in engine power begins.

Values of $\Delta\eta_v$ obtained from figure 9 are plotted against $v_d n/A$ for constant values of p_o/p_m in figure 11. A comparison of figures 10 and 11 shows that, as $v_d n/A$ is increased, a loss in engine power occurs before there is a loss in volumetric efficiency. The values of $\Delta\phi$ and $\Delta\eta_v$ at $p_o/p_m = 0.2$ were obtained by extrapolating the curves in figures 8 and 9.

The foregoing discussion also applies in general to the 90° bend and the 180° bend, which gave results similar to those obtained for the S-shaped stack. The various curves for the 90° and 180° bends are given in the following figures:

	90° bend	180° bend
$\overline{V}_e$ against $p_o A/M_e$	--	4(a)
$v_d n/A$ against p_o/p_m	5(b)	5(c)
$(\overline{V}_e)_{eff}$ against $p_o A/M_e$	6(b)	6(c)
ϕ against p_o/p_m	12	16
η_v against p_o/p_m	13	--
$\Delta\phi$ against $v_d n/A$	14	17
$\Delta\eta_v$ against $v_d n/A$	15	--

The curves of η_v and $\Delta\eta_v$ for the 180° bend have been omitted in order to reduce the number of figures.

The maximum net gain in thrust horsepower for a given set of conditions is approximately the same for these three stacks, although the required nozzle area will vary slightly for the different stacks.

A comparison of figures 8, 12, and 16 with the corresponding curves for the 25-inch straight stack show that corresponding values of ϕ for the unrestricted stack condition agree fairly well. The disagreement is greatest at low engine speeds and at $p_o/p_m = 1.0$. Since the scatter appears to be random, it is believed to be due to experimental error and to changes in the engine, which was overhauled several times during the tests.

The Effect of Stack Length on Engine Power

The 44-inch straight stack.- The values of ϕ and $\Delta\phi$ for a straight exhaust stack 44 inches long are shown in figures 18 and 19, respectively. The scatter of data makes it difficult to determine how $\Delta\phi$ varies in the region where a loss in power begins (fig. 19). A critical value of $v_d n/A$ was obtained by fairing two straight lines through each plot and considering the point of intersection at $\Delta\phi = 0$ as the critical value. A similar treatment was made (reference 1) for the 25-inch stack. The apparent value of $v_d n/A$ at which a loss in engine power just occurs is much higher for these straight stacks than for bent stacks, but the transition to the region of power loss is much sharper for straight stacks.

The critical values of $v_d n/A$ for the 44-inch and the 25-inch straight stacks are shown in figure 5(d). The differences between the critical values of $v_d n/A$ for these two stacks are well within the limits of probable experimental error. The values of ϕ_o at corresponding conditions are approximately the same for the two stack lengths; thus, no change in engine power may be attributed to the increase in stack length on the basis of the available data. No other effect on the performance of the jet-propulsion system is to be expected with the 44-inch stack.

As the exhaust stack length is increased, the effects of gas friction will tend to create higher mean pressures in the cylinder during the time that its volume is decreasing

with a resulting loss in power. Resonance effects also become more important as the stack length increases. It is evident that there is a limit to the length of exhaust stack that may be used without an appreciable effect on power.

The 108-inch straight stack.- A straight exhaust stack 108 inches long was tested for its effect on engine power. Figure 20 shows the variation of ϕ with engine speed for various nozzle areas and at values of p_o/p_m equal to 0.4, 0.7, and 1.0. Corresponding curves are shown for the 25-inch stack at $p_o/p_m = 0.4$ and 0.7. The curves for $p_o/p_m = 1.0$ are not given for the 25-inch stack because of excessive scatter of the data.

The effects of resonance between the natural frequency of pressure waves in the exhaust system and engine speed are appreciable and no correlation is obtained by plotting ϕ and $\Delta\phi$ against p_o/p_m and $v_d n/A$, respectively. The long stack was found to have an adverse effect on engine power for most practical combinations of engine speed and nozzle area.

As the ratio p_o/p_m decreases, the volume rate of flow in the stack increases and the acoustic velocity is maintained at the nozzle exit for a longer period of time. No pulses being reflected in a gas stream moving at the velocity of sound, the effects of resonance tend to decrease with p_o/p_m. The difference in ϕ for the long and the short stacks is then mainly due to the larger pressure drops required by gas friction in the long stack. When a nozzle is placed on the stack, pulses will be reflected by the surface representing the difference between stack area and nozzle exit area; thus, when the flow from the nozzle is mainly acoustic, resonance will occur with small nozzles and will tend to decrease as the nozzle exit area increases. The effects of a decrease in p_o/p_m and an increase in nozzle area may be seen by inspection of figure 20.

The Effect of a Branched Stack on Engine Power

The variation of ϕ and $\Delta\phi$ with p_o/p_m and $v_d n/A$, respectively, are shown for the branched stack in figures 21 and 22. The values of ϕ_o agree fairly well

with corresponding values for the stacks previously discussed. The critical values of $v_d n/A$ are shown in figure 5(e).

Although these tests of a single-cylinder engine indicate that the branched stack has no adverse effects on engine power, it is not certain that this result will be true when both legs of the stack are being used.

For example, it is known that if the two legs are connected to cylinders having an appreciable overlap in exhaust valve timing, a loss in power will result. Further investigation with branched stacks on multicylinder engines is required before an accurate prediction of their effect on engine power can be made.

CONCLUSIONS

Based on test-stand measurement of exhaust-gas jet thrust and engine power for an 1820-G cylinder it is concluded that:

1. The mean exhaust-gas jet velocity obtained with individual exhaust stacks was not appreciably changed by the addition of smooth bends to the exhaust stack or by changes in length up to at least 4 feet. The curve previously obtained for the 25-inch straight stack may be used to predict the thrust obtainable with stacks falling in the foregoing classification.

2. The presence of smooth bends in individual exhaust stacks having no nozzle restriction had no appreciable effect on engine power, although a loss in engine power occurred for less reduction in nozzle area with bent stacks than with straight stacks.

3. The maximum total performance obtainable was not greatly affected by the use of bent stacks, although the correct nozzle area varied with the amount of bend employed.

4. Increases of stack length up to 44 inches had no effect on engine power; a stack 108 inches long had an adverse effect on engine power for most practical combinations of nozzle exit area and engine speed.

Langley Memorial Aeronautical Laboratory,
National Advisory Committee for Aeronautics,
Langley Field, Va.

REFERENCE

1. Pinkel, Benjamin, Turner, L. Richard, and Voss, Fred: Design of Nozzles for the Individual Cylinder Exhaust Jet Propulsion System. NACA ACR, April 1941.

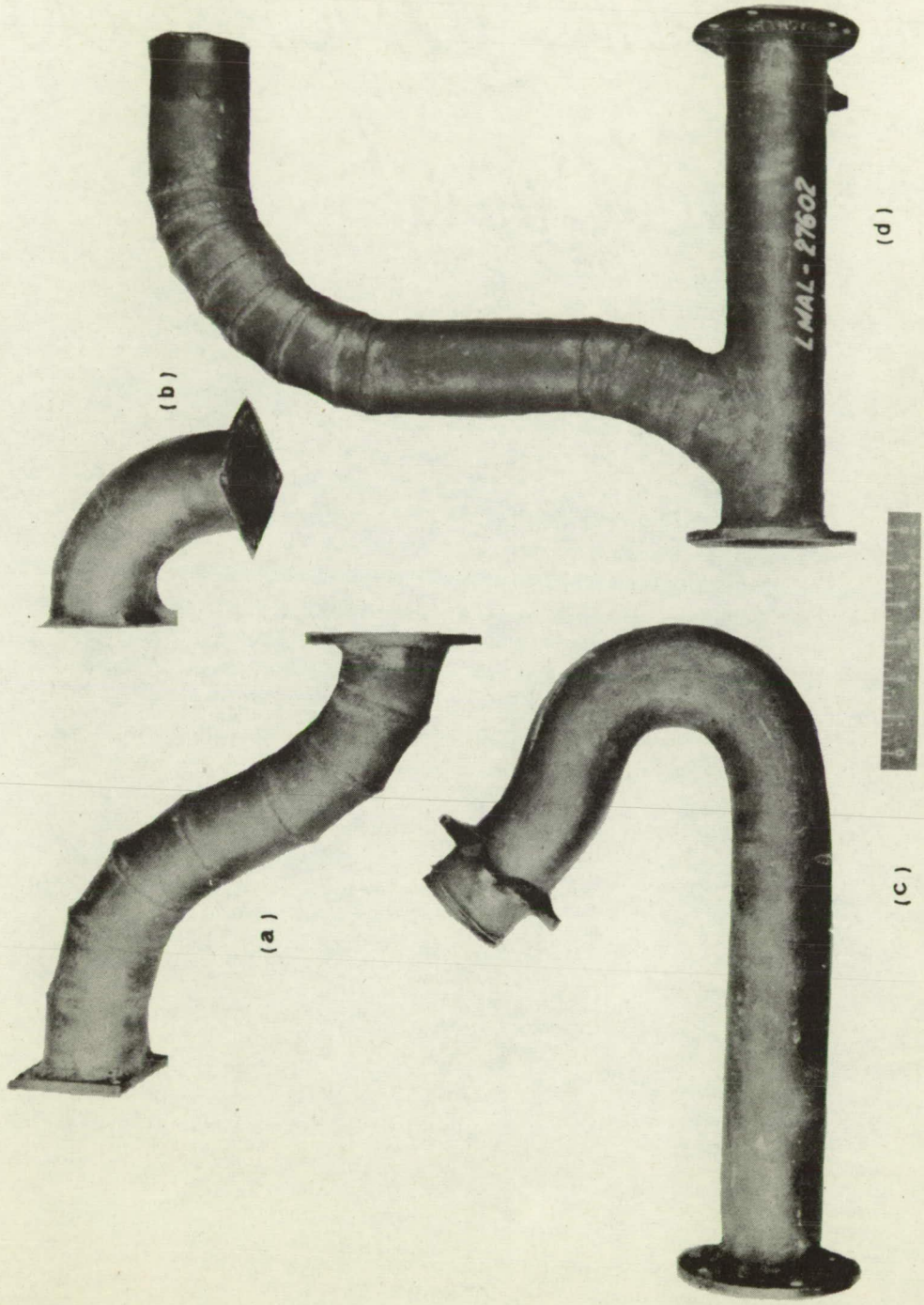

Figure 1. - Four of the stacks tested.

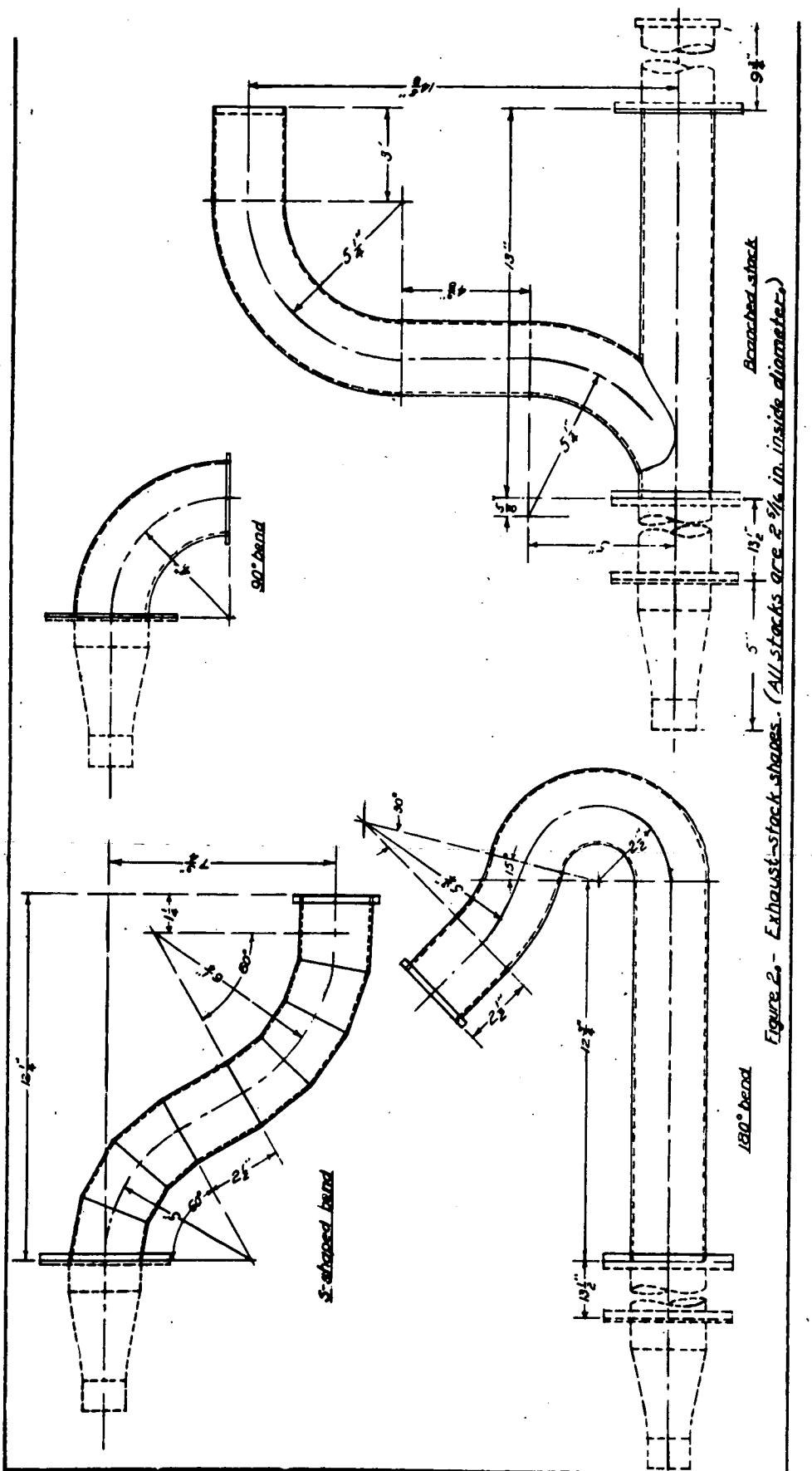

Figure 2.- Exhaust-stack shapes. (All stacks are 2 5/16 in. inside diameter.)

Figure 3. - The seven nozzles tested.

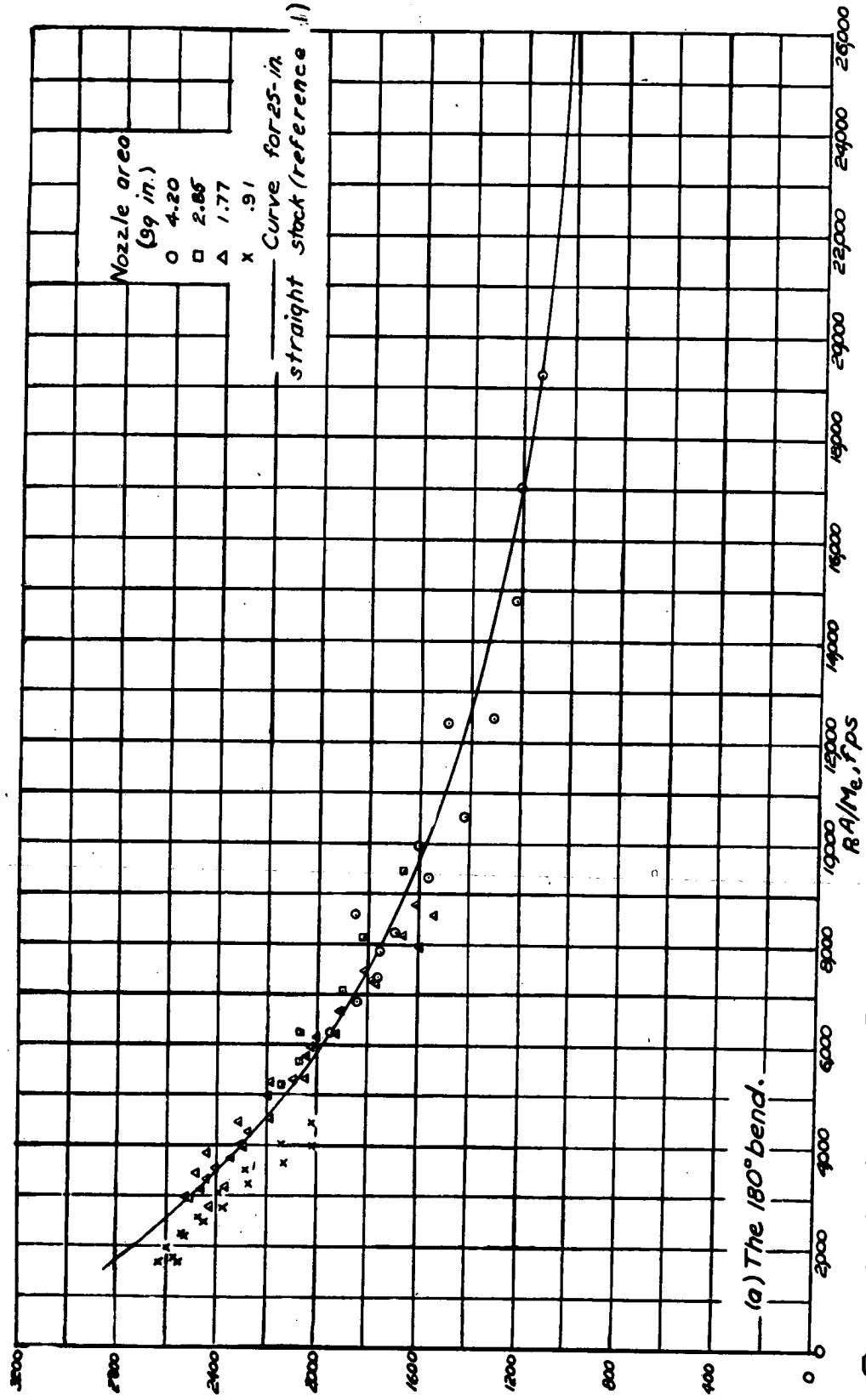

Figure 4.- Variation of $\overline{V}_e$ with $\rho_2 A/M_e$.

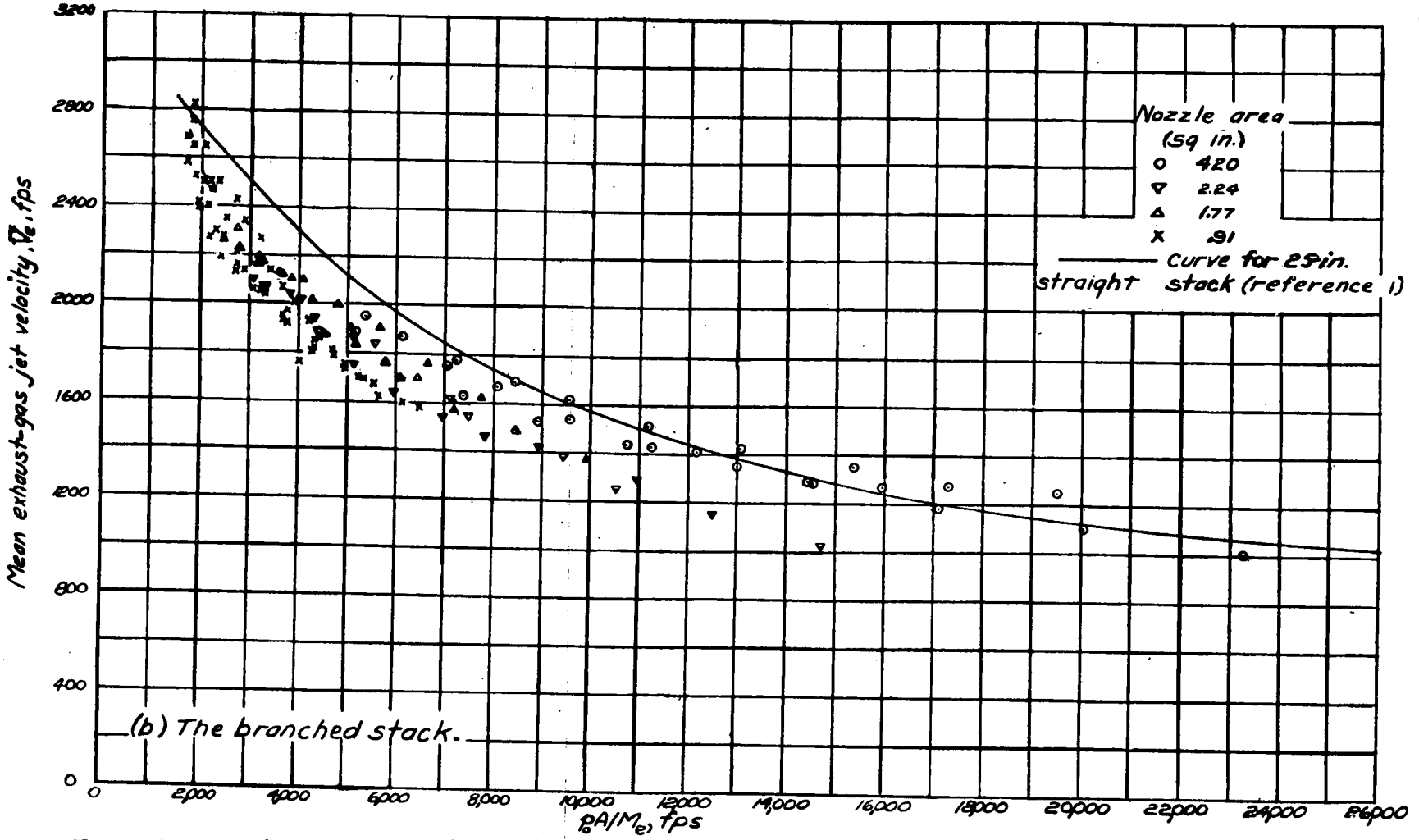

Figure 4.- Continued. Variation of $\overline{V}_e$ with $p_o A/M_e$.

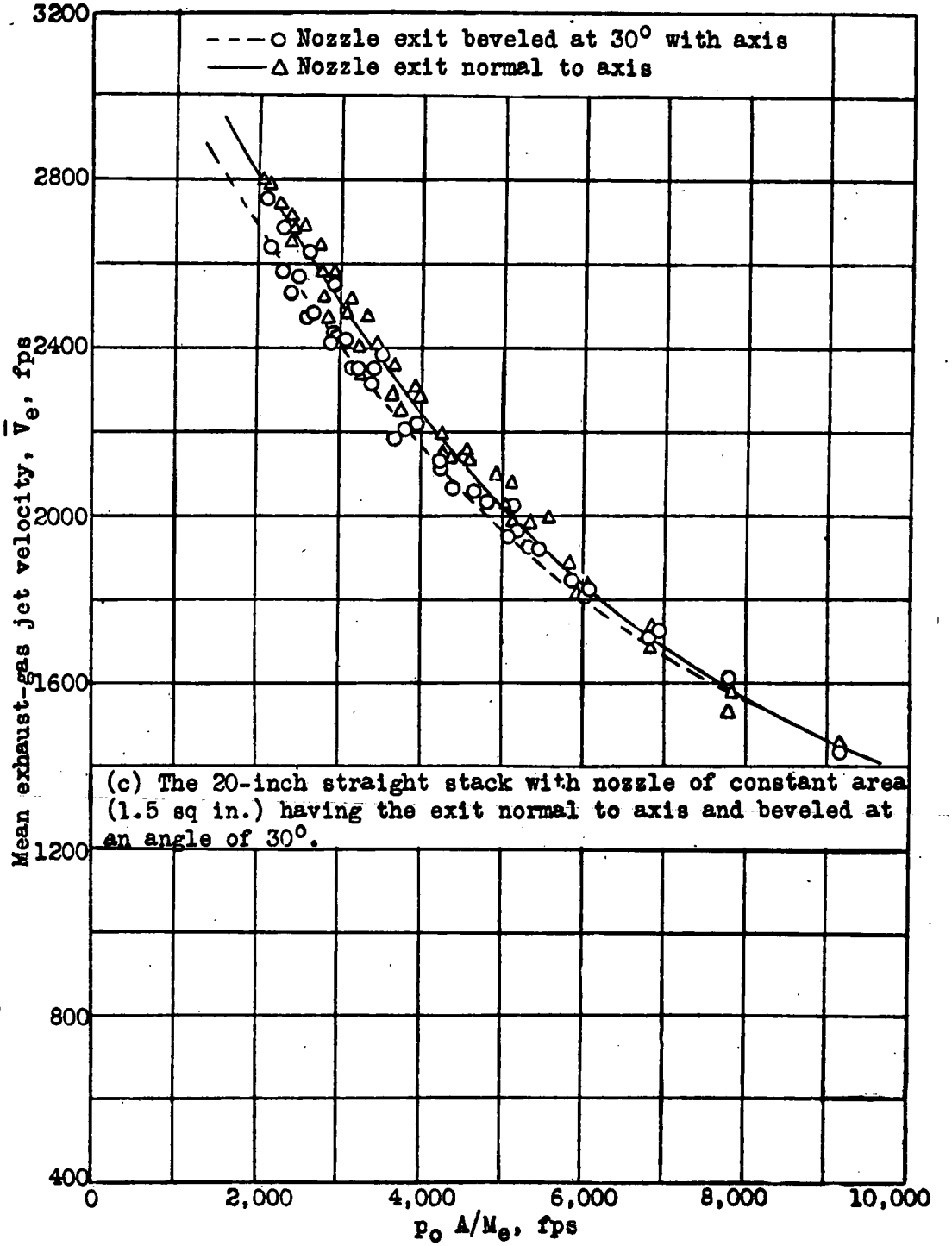

Figure 4.- Concluded. Variation of $\bar{V}_e$ with $p_o A/M_e$.

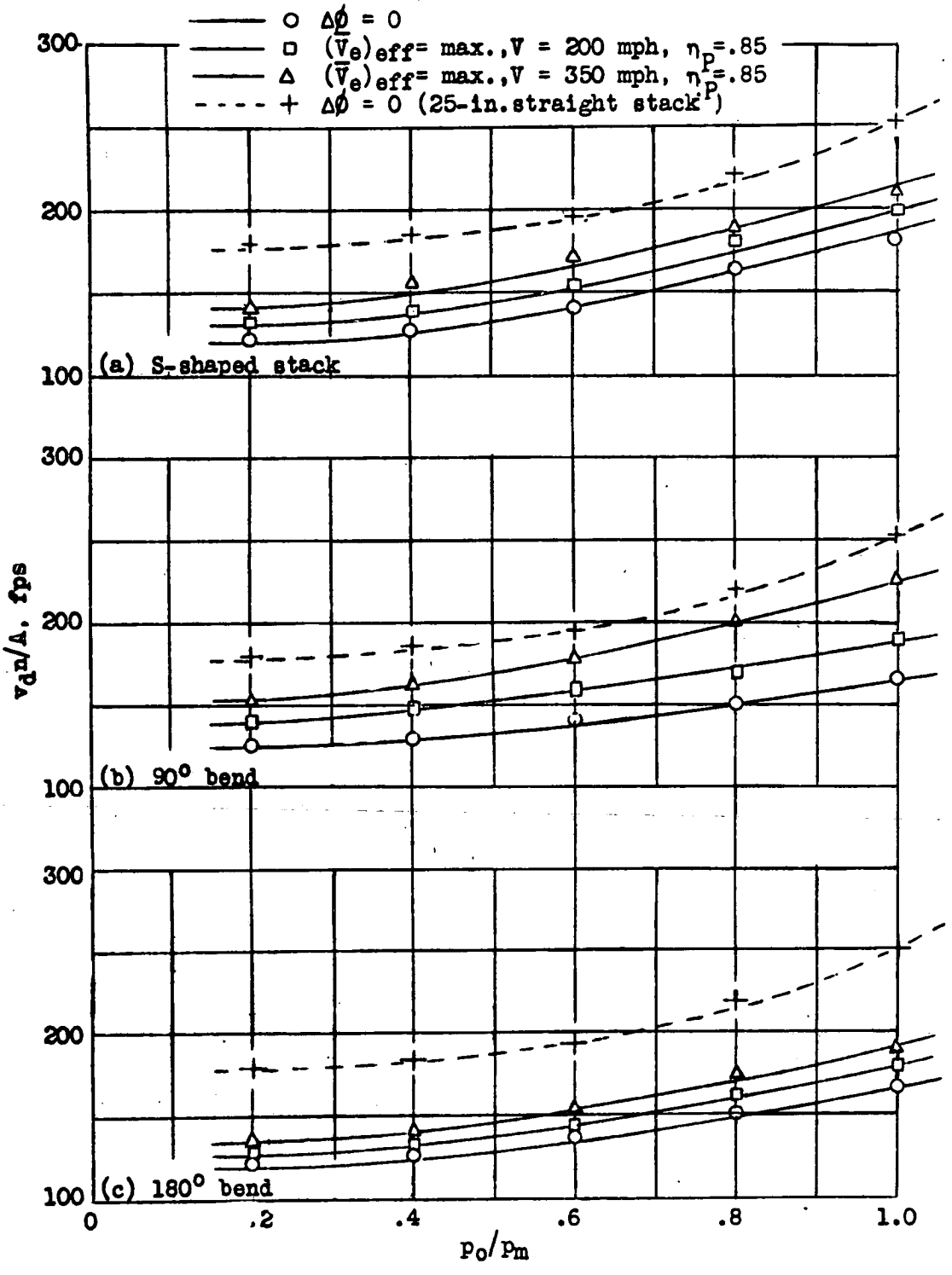

Figure 5.- Variation of optimum values of $v_d n/A$, with p_o/p_m.

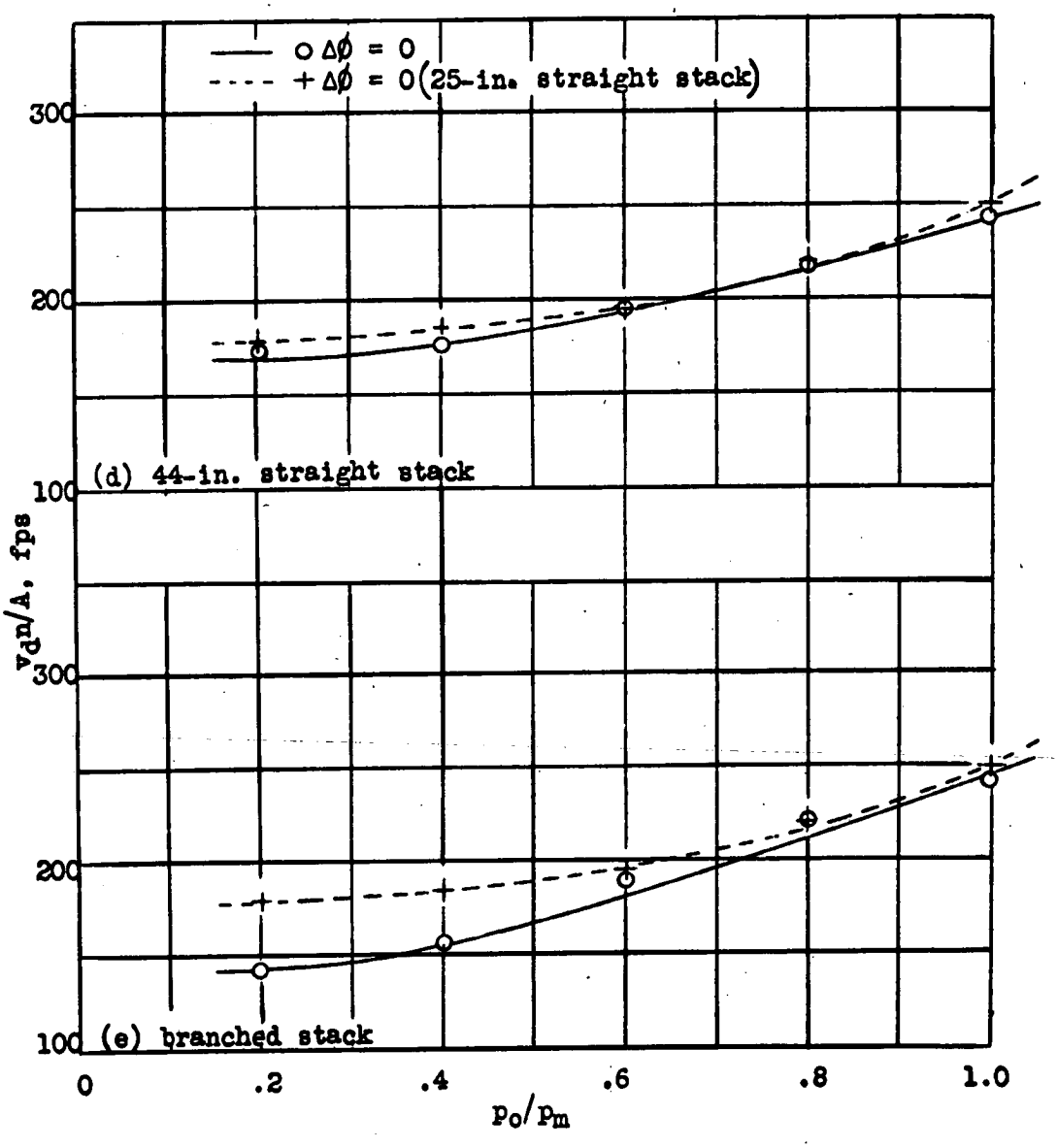

Figure 5.- Concluded. Variation of optimum values of $v_d n/A$ with p_o/p_m.

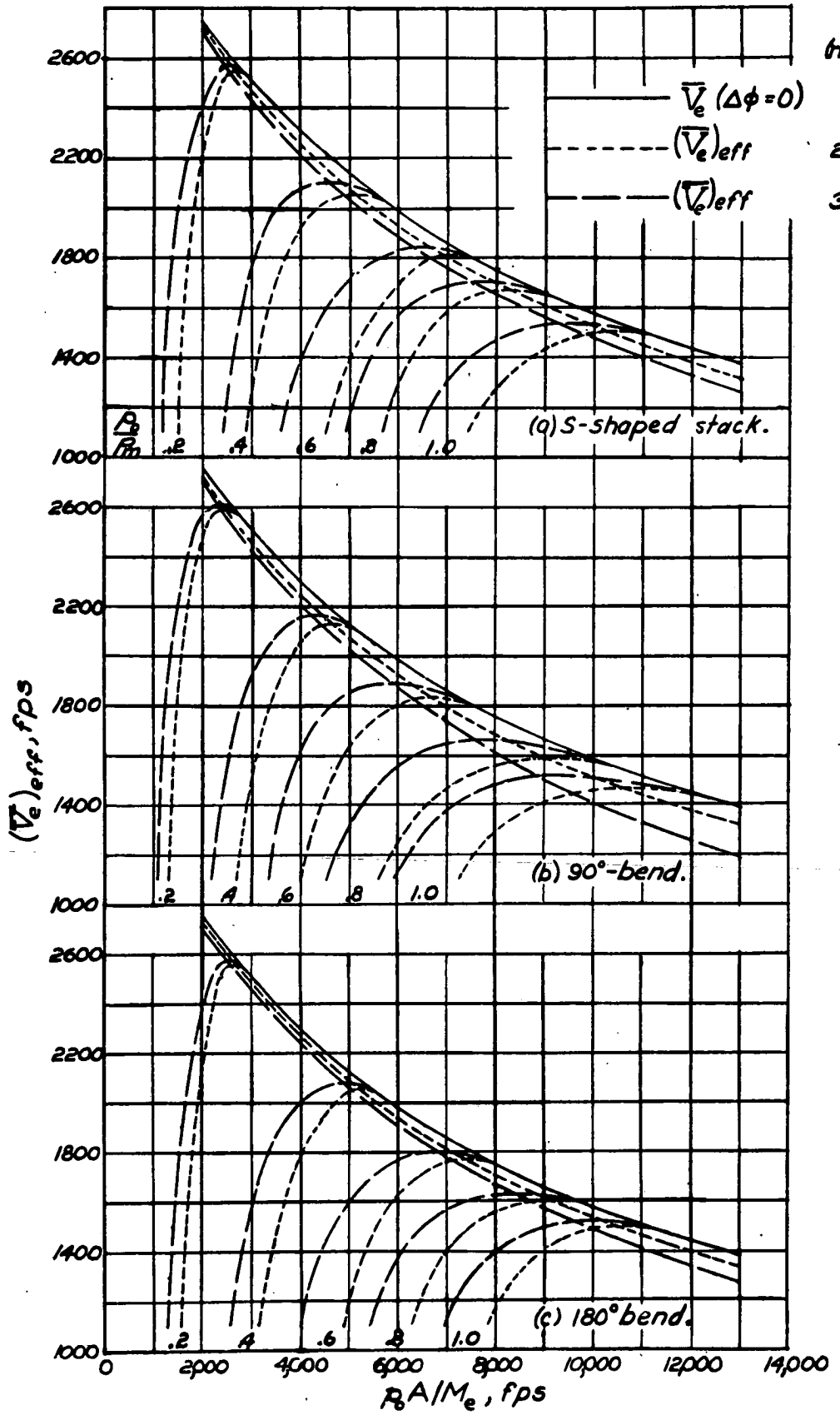

Figure 6.- Variation of $(\overline{V}_e)_{eff}$ with $p_o A/M_e$.

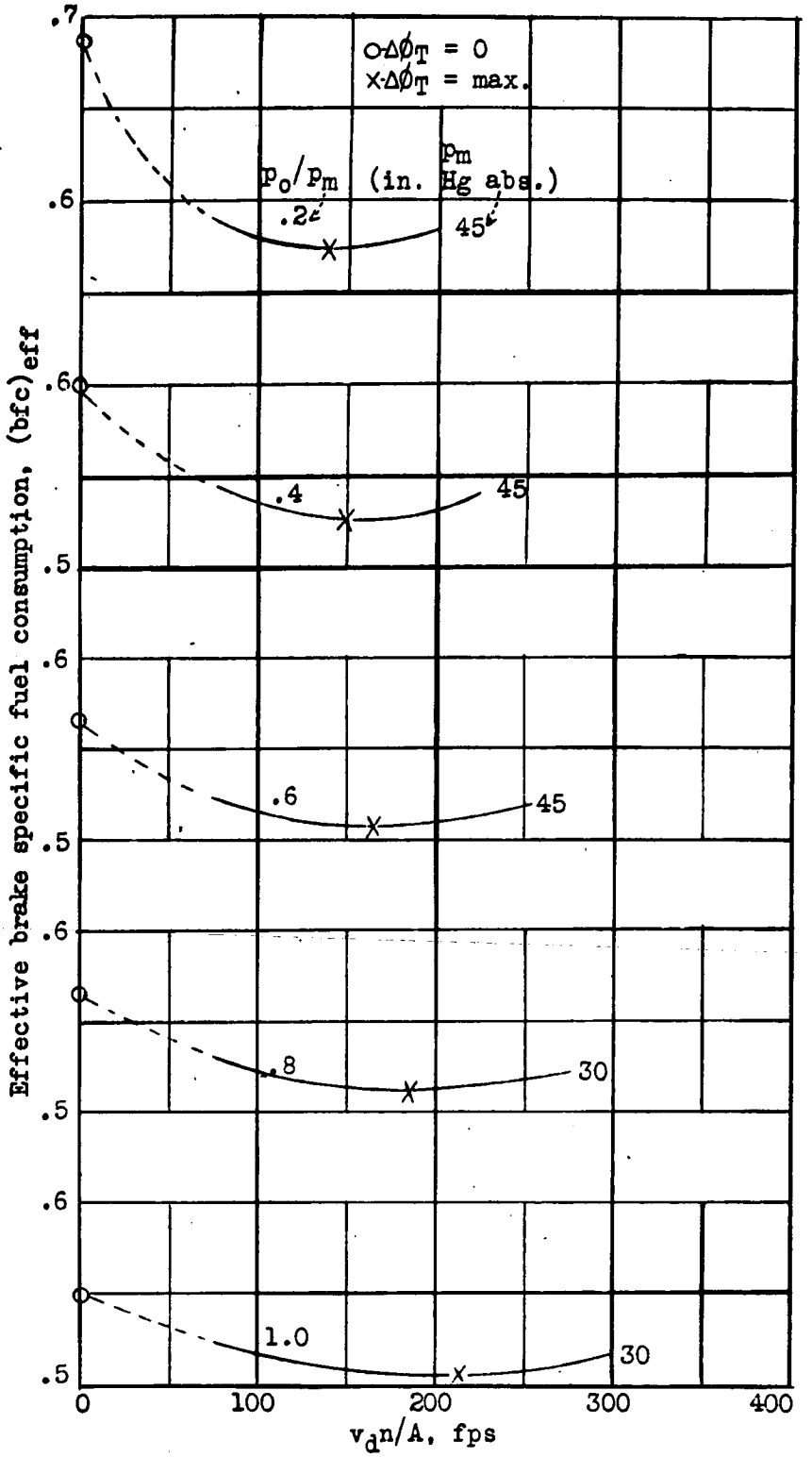

Figure 7.- Variation of effective brake specific fuel consumption with $V_d n/A$ for stack having S-shape, Airplane velocity = 350 miles per hour; $\eta_p = .85$.

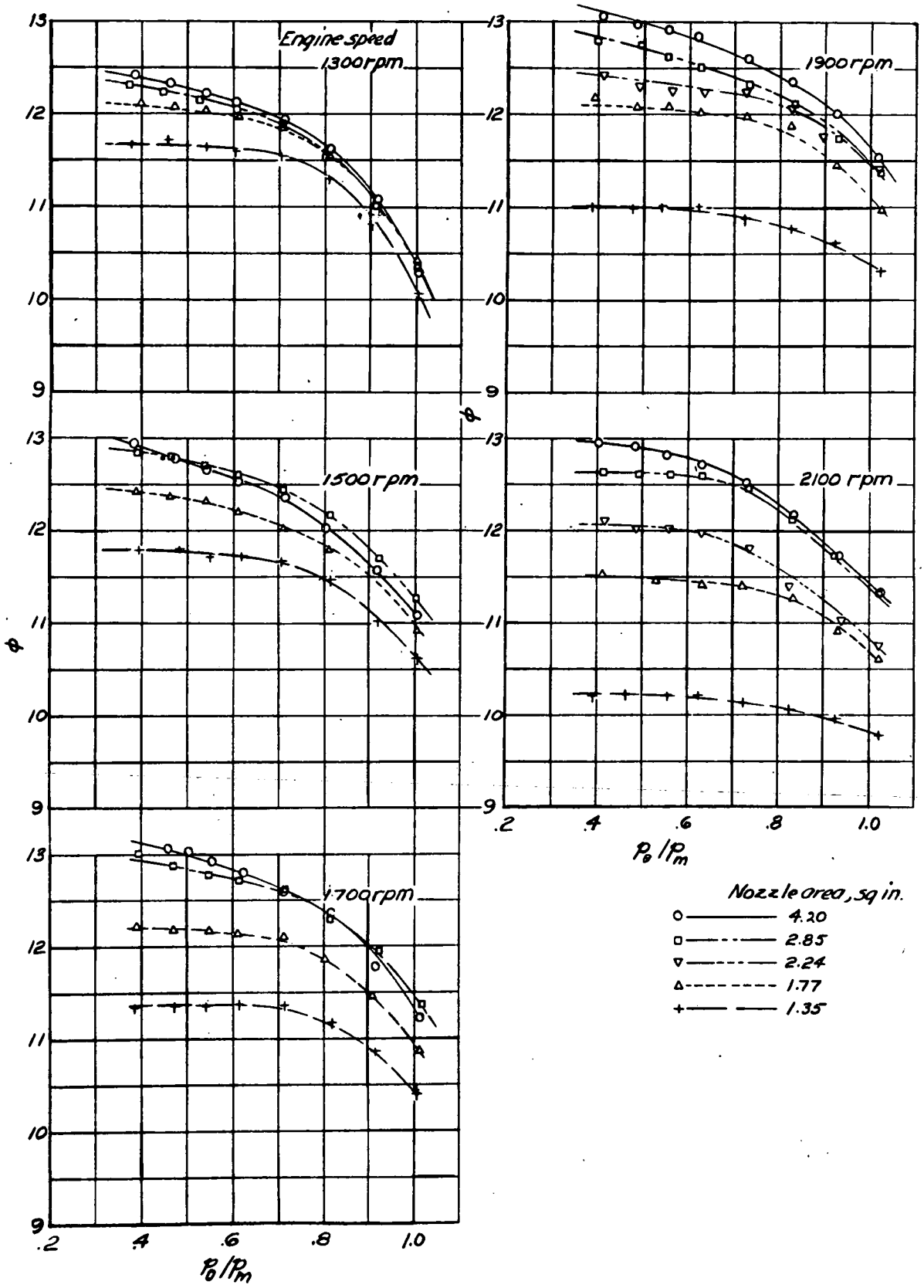

Figure 8. – Variation of ϕ with p_o/p_m and nozzle area at constant engine speeds for stack having S-shape.

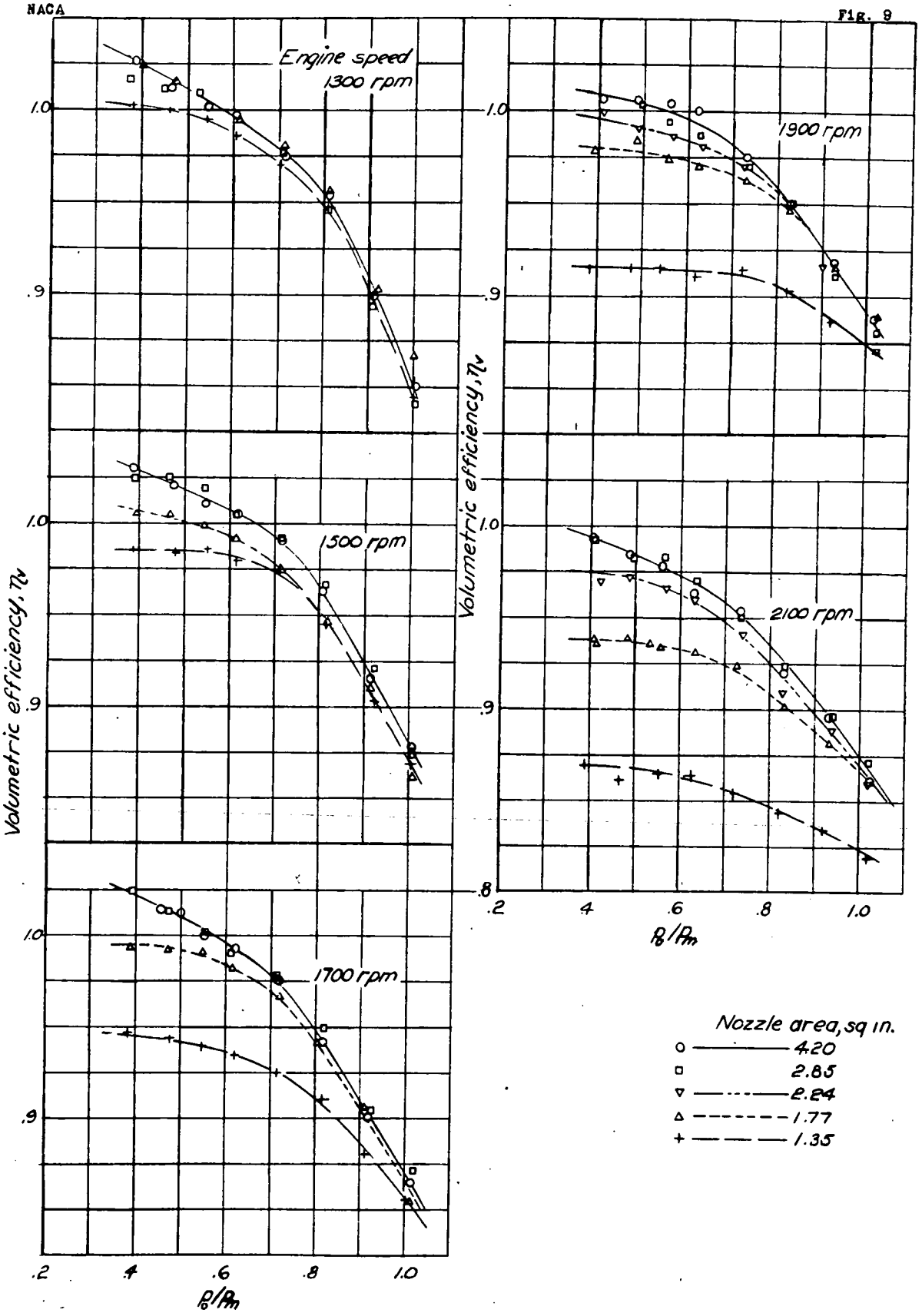

Figure 9.—Variation of volumetric efficiency η_v with p_b/p_m and nozzle area at constant engine speeds for stack having S-shape.

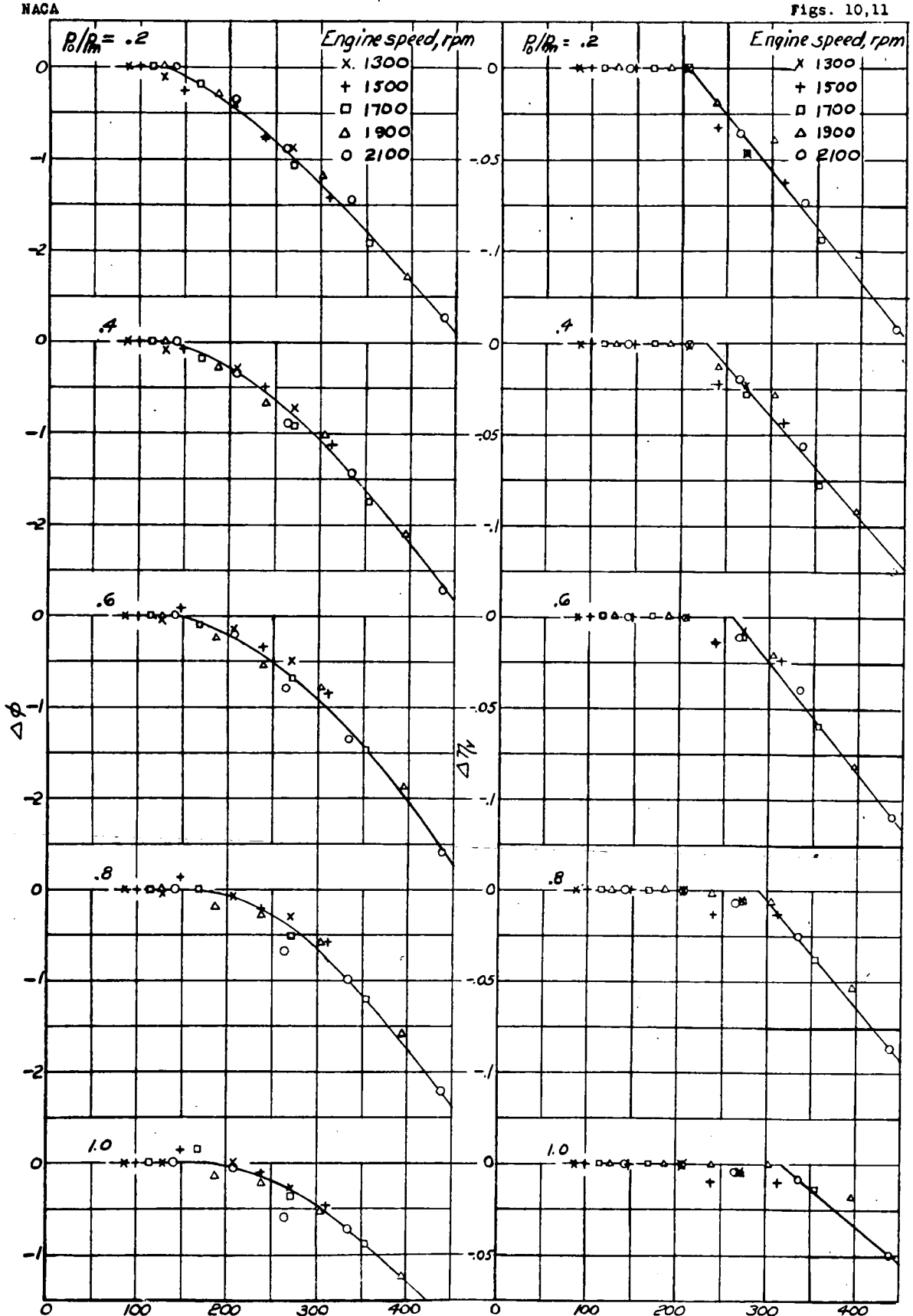

Figure 10.- Variation of $\Delta\phi$ with $v_d n/A$ for stack having S-shape.

Figure 11.- Variation of $\Delta\eta_v$ with $v_d n/A$ for stack having S-shape.

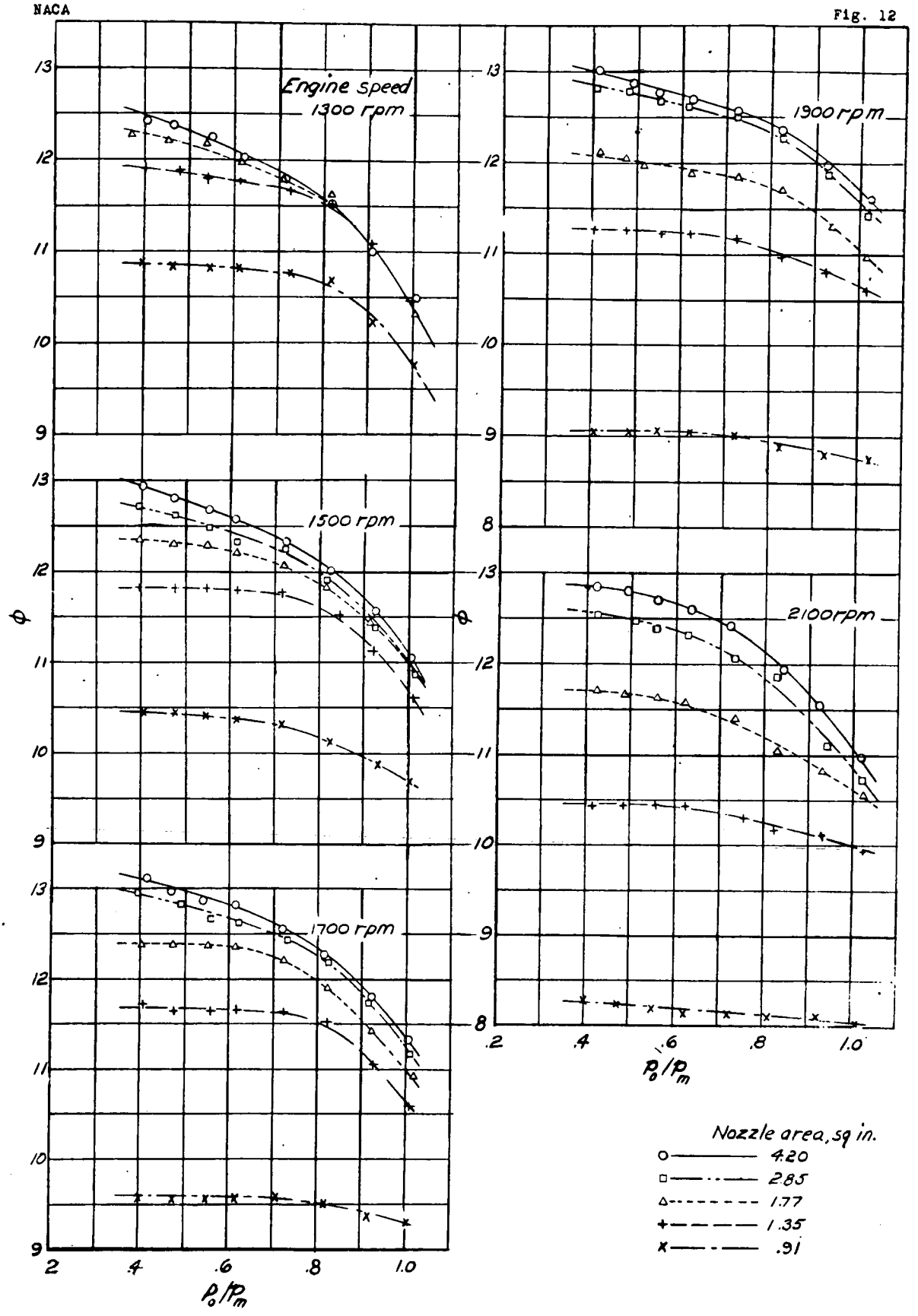

Figure 12.–Variation of ϕ with p_o/p_m and nozzle area at constant engine speeds for stack having 90° bend.

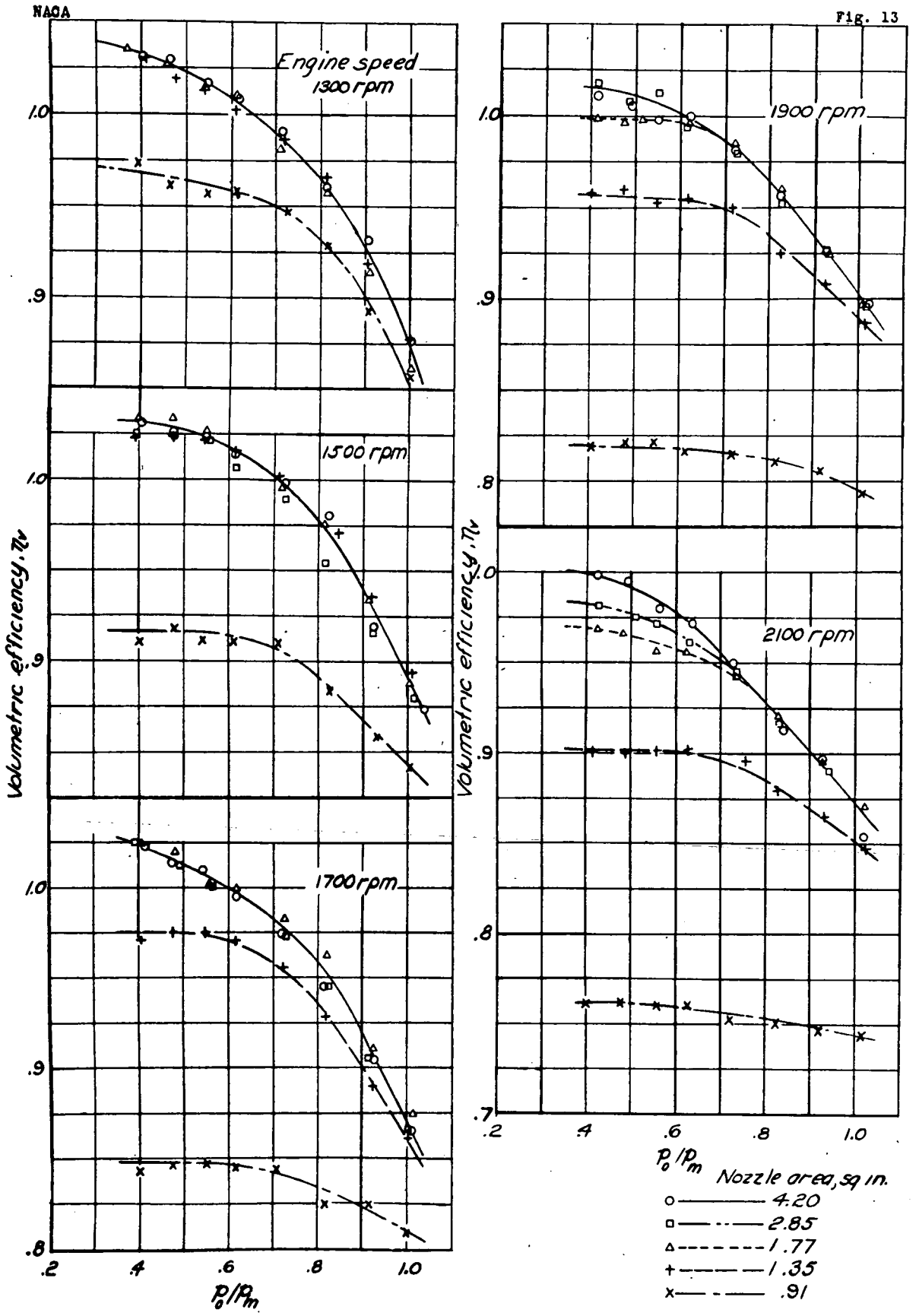

Figure 13.- Variation of volumetric efficiency η_v with p_0/p_m and nozzle area at constant engine speeds for stack having 90° bend.

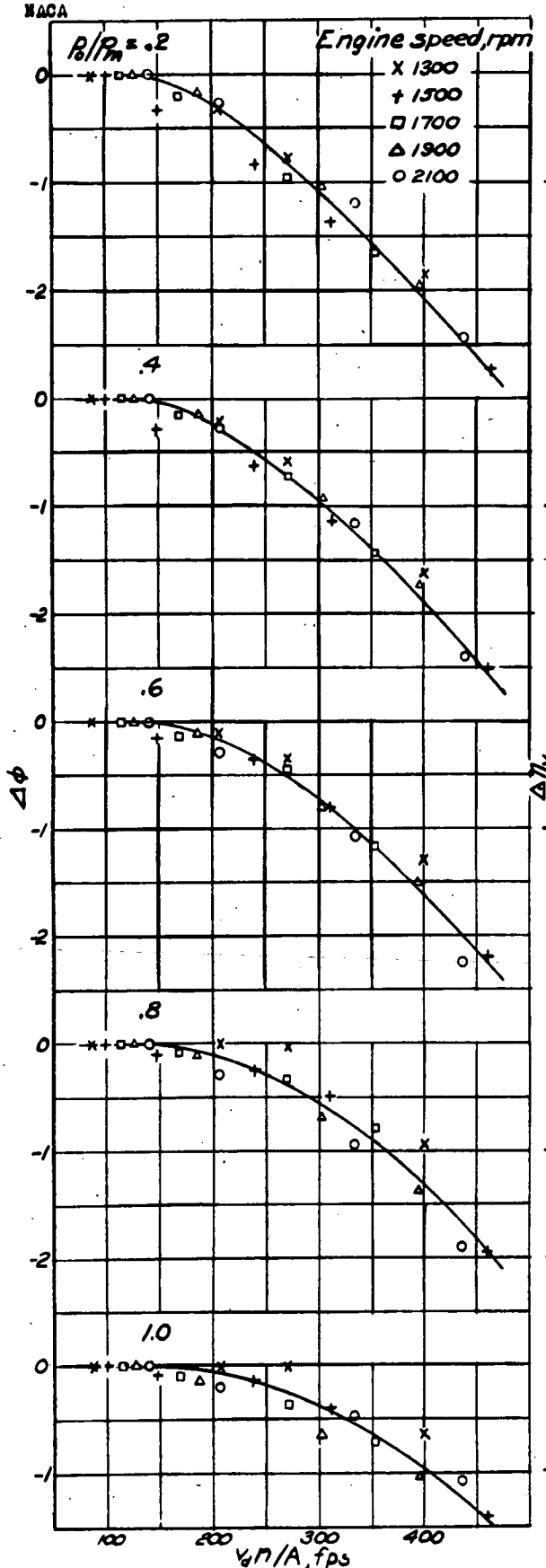

Figure 14.-Variation of $\Delta\phi$ with $V_e n/A$ for stack having 90° bend.

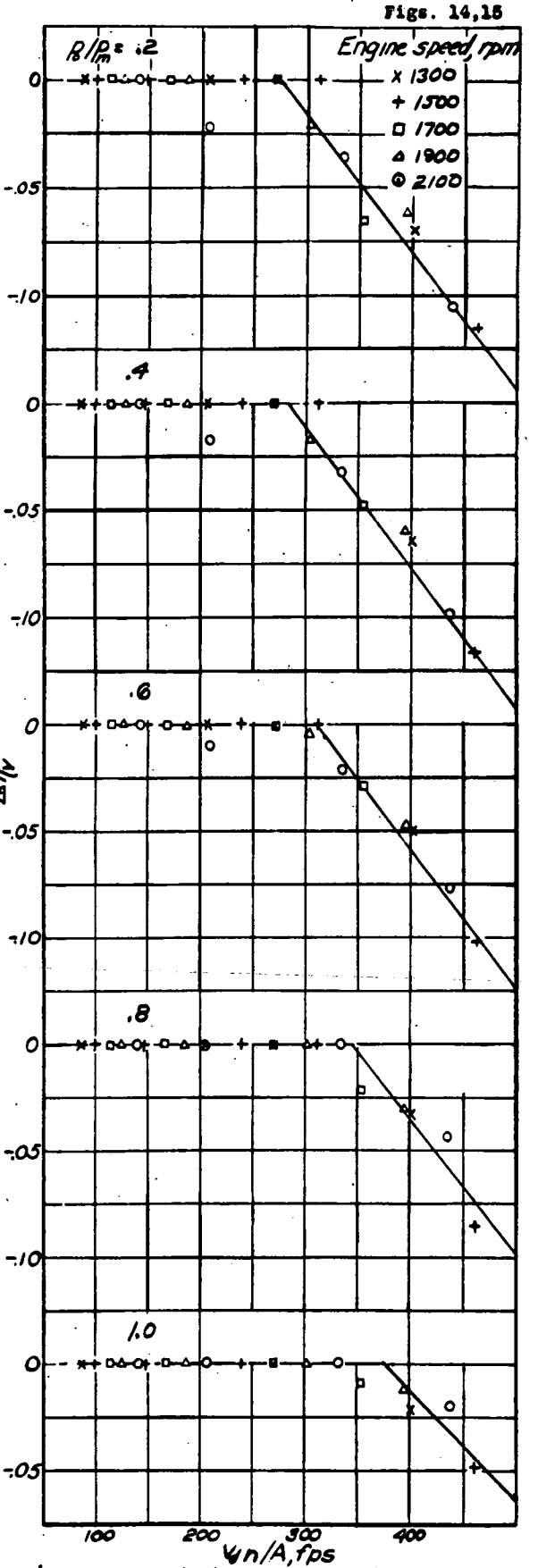

Figure 15.-Variation of $\Delta\eta_v$ with $V_e n/A$ for stack having 90° bend.

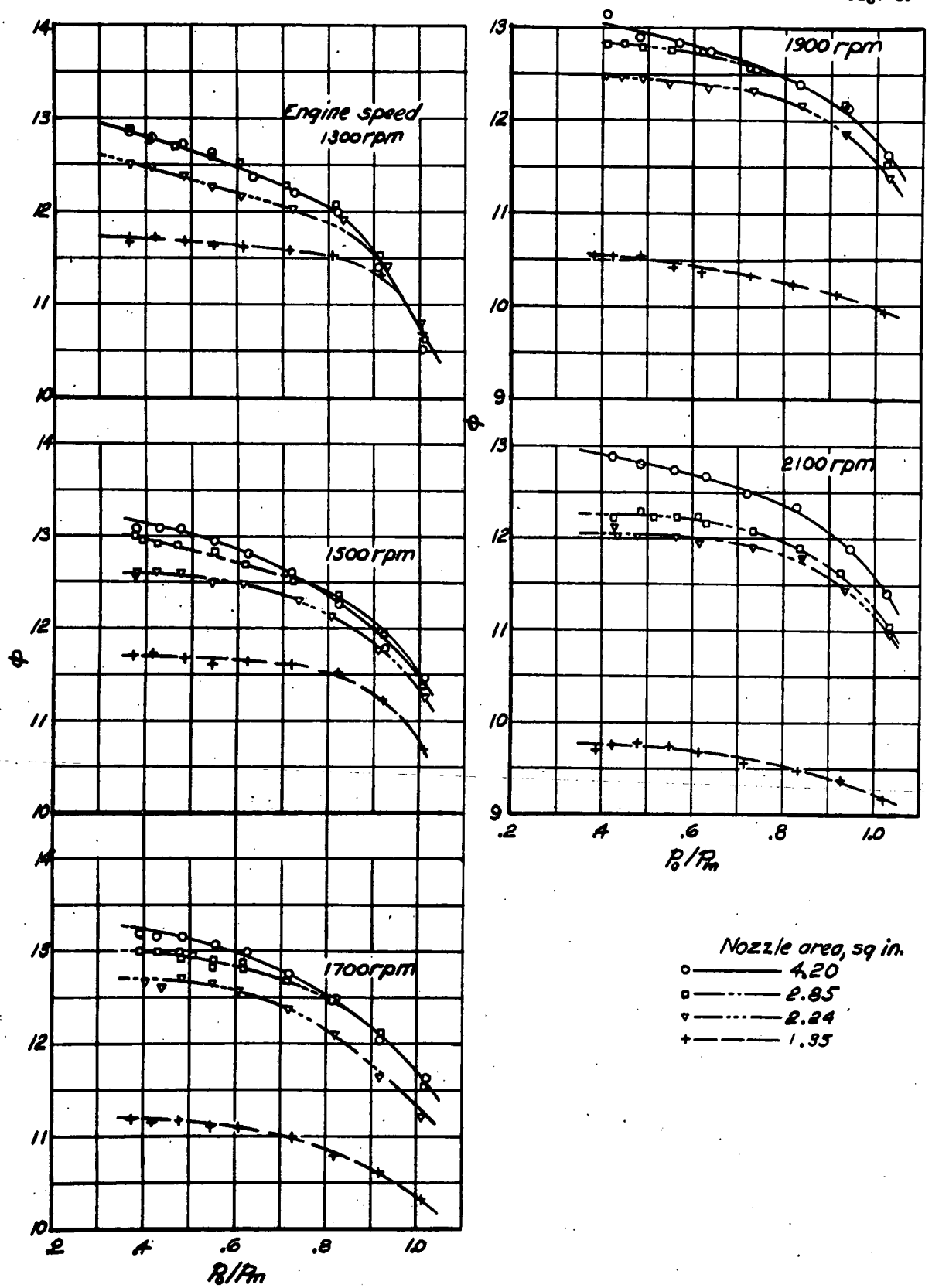

Figure 16.- Variation of ϕ with P_0/P_m and nozzle area at constant engine speeds for stack having 180° bend.

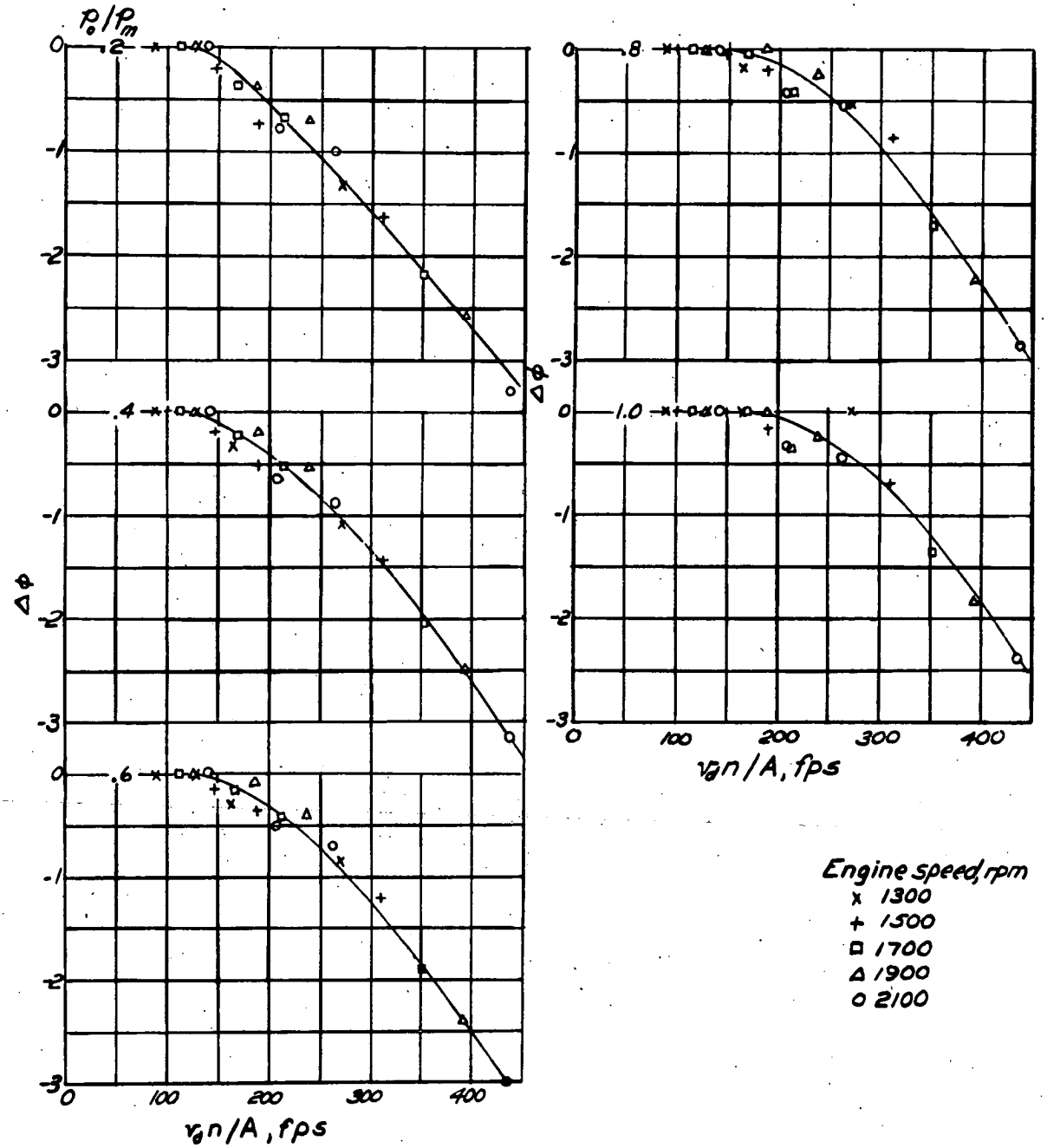

Figure 17.- Variation of $\Delta\phi$ with $v_d n/A$ for stack having 180° bend.

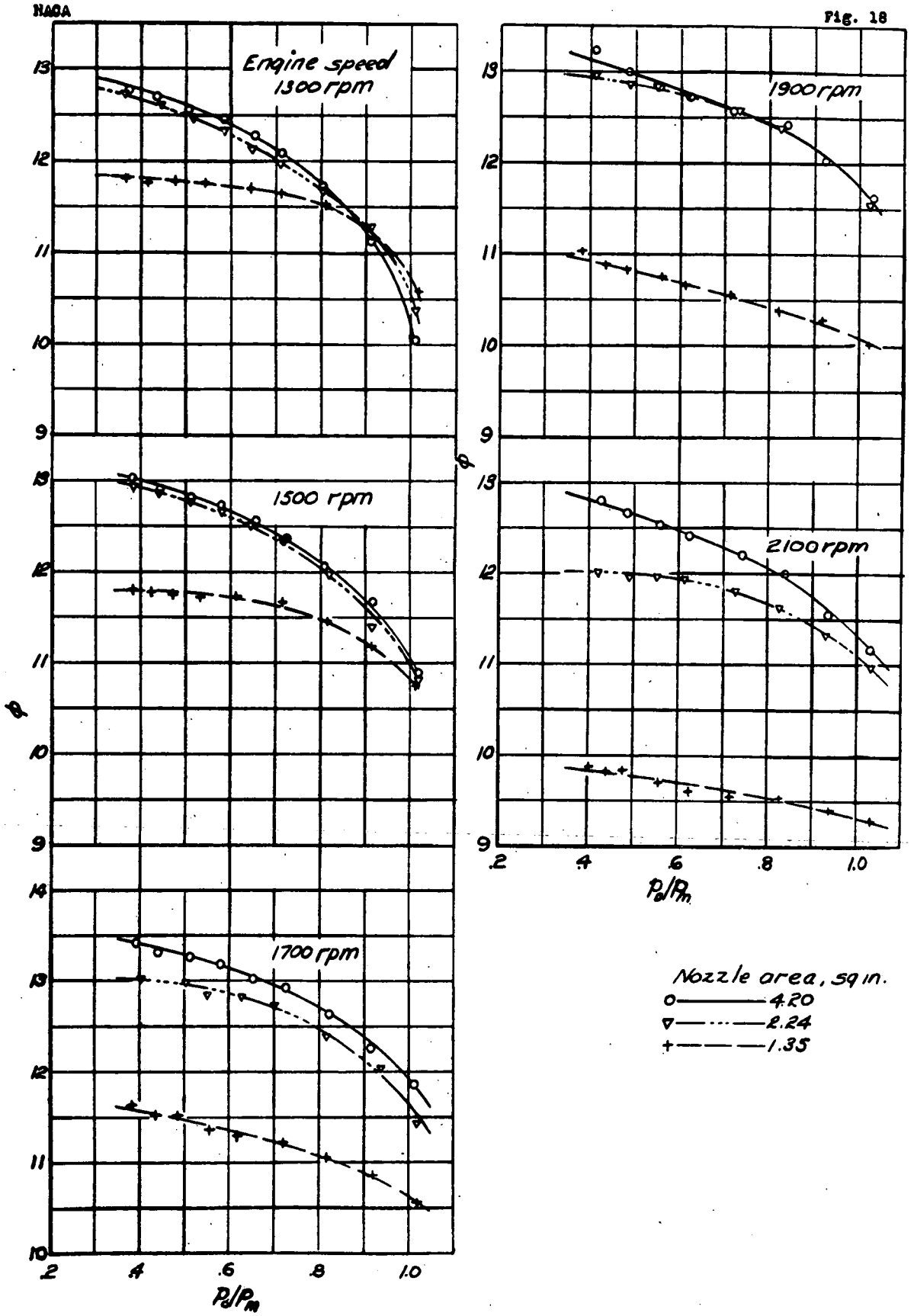

Figure 18.-Variation of ϕ with p_d/p_m and nozzle area at constant engine speeds for 44-inch straight stack.

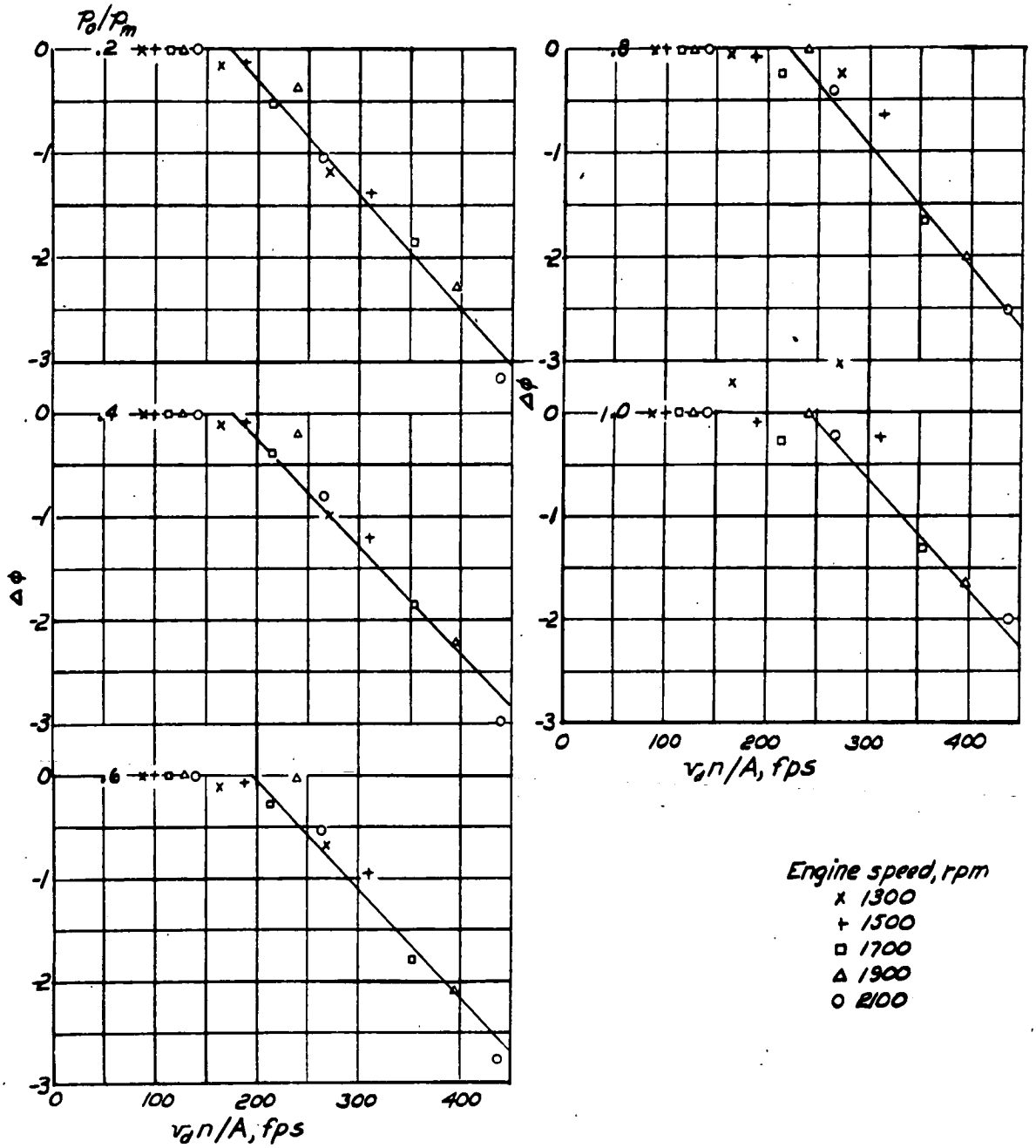

Figure 19.- Variation of $\Delta\phi$ with $v_0 n/A$ for 44-inch straight stack.

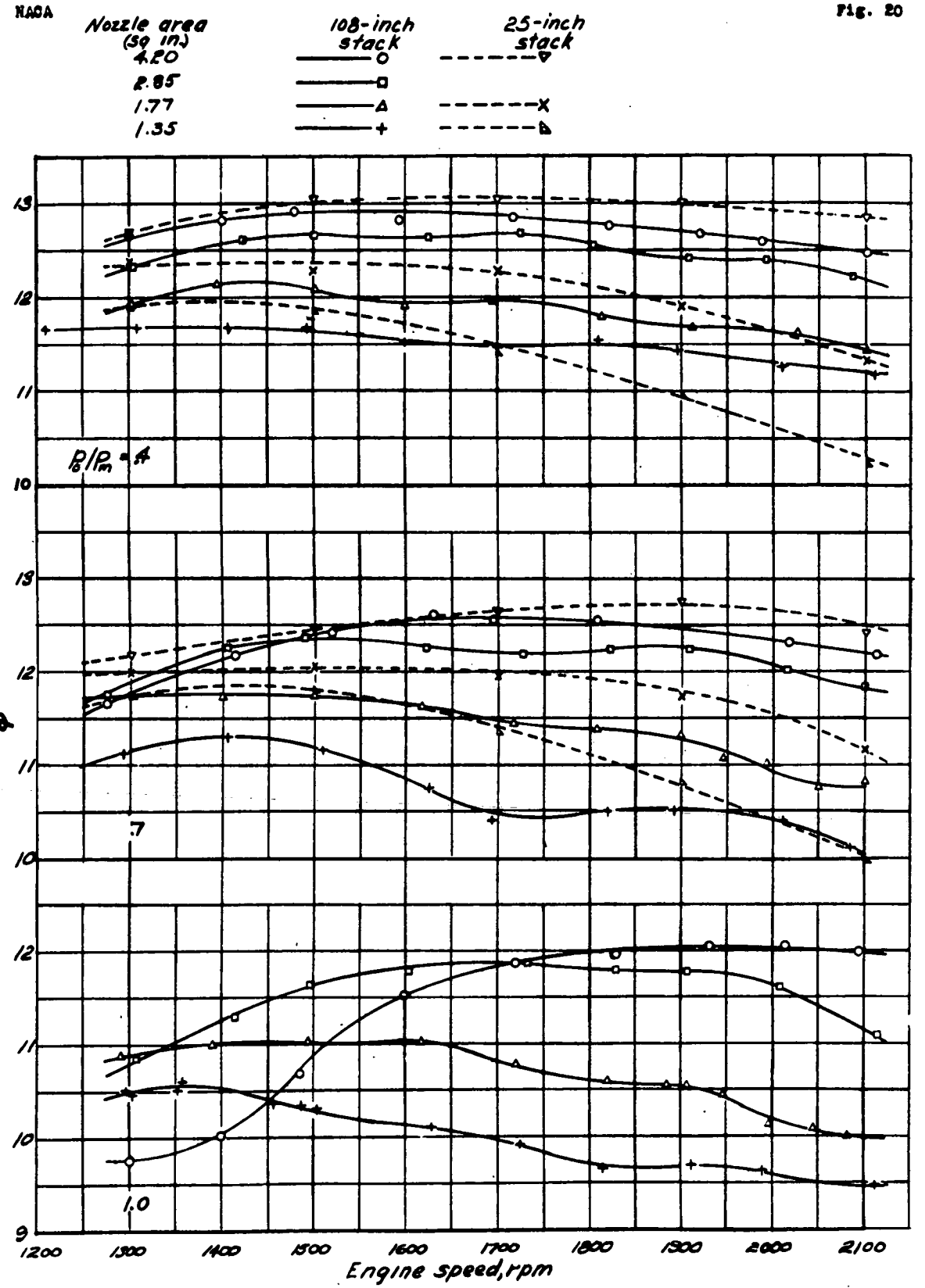

Figure 20.-Variation of ϕ with engine speed and nozzle area at constant values of P_b/P_m for 108-inch stack and 25-inch stack.

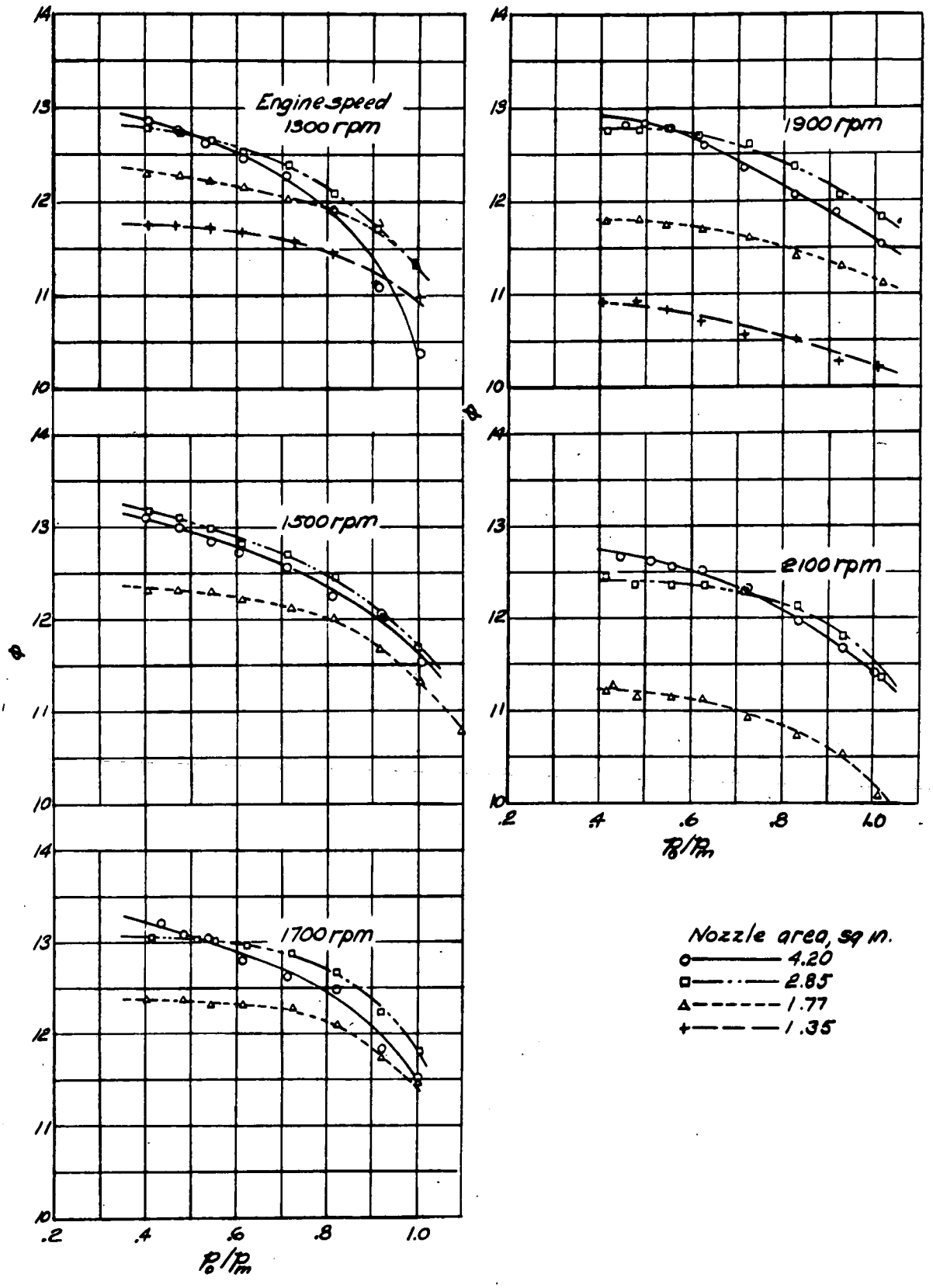

Figure 21.- Variation of ϕ with p_b/p_m and nozzle area at constant engine speeds for branched stack.

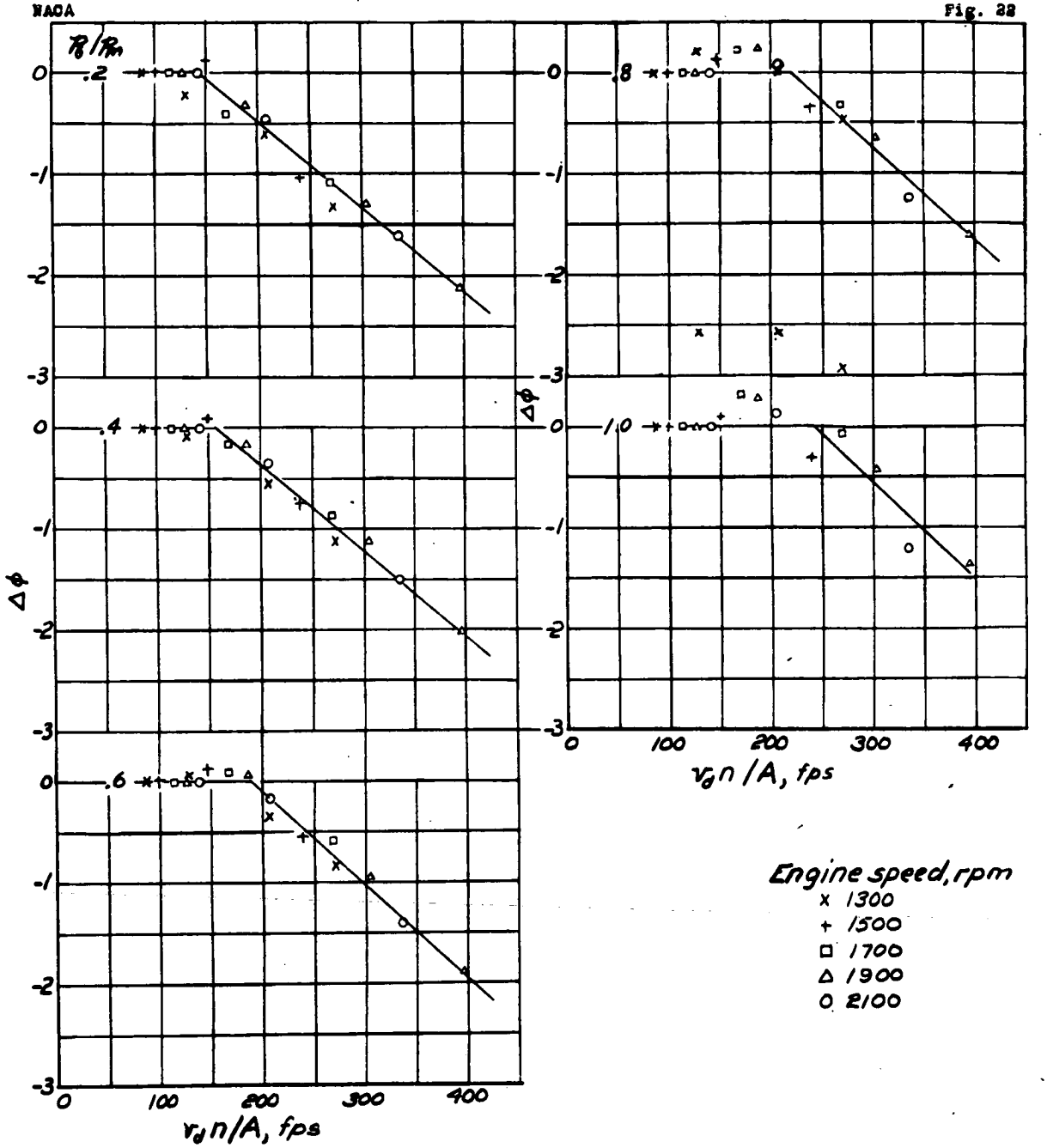

#21

Figure 22.- Variation of $\Delta\phi$ with $v_d n/A$ for branched stock.